



Impact of recycled plastic content on bond line performance

An investigation into how recycled polypropylene affects adhesion between plastic components in electric vehicle batteries.

Master's thesis in Materials Chemistry

LOUISA EÉN
WILMA JÖNSSON

MASTER'S THESIS 2025

Impact of recycled plastic content on bond line performance

An investigation into how recycled polypropylene affects adhesion between plastic components in electric vehicle batteries.

LOUISA EÉN
WILMA JÖNSSON



CHALMERS
UNIVERSITY OF TECHNOLOGY

Department of Chemistry and Chemical Engineering
CHALMERS UNIVERSITY OF TECHNOLOGY
Gothenburg, Sweden 2025

Impact of recycled plastic content on bond line performance

An investigation into how recycled polypropylene affects adhesion between plastic components in electric vehicle batteries.

LOUISA EÉN, WILMA JÖNSSON

© LOUISA EÉN, WILMA JÖNSSON, 2025.

Supervisor: Kerstin Wasmuth, Volvo Cars Corporation

Examiner: Magnus Skoglundh, Department of Applied Chemistry at Chalmers University of Technology

Master's Thesis 2025

Department of Chemistry and Chemical Engineering

Chalmers University of Technology

SE-412 96 Gothenburg

Sweden

Telephone +46 31 772 1000

Cover: Visualisation of Volvo's SPA3 battery package, adapted from an animation made by Volvo [1].

Typeset in L^AT_EX

Gothenburg, Sweden 2025

Impact of recycled plastic content on bond line performance

An investigation into how recycled polypropylene affects adhesion between plastic components in electric vehicle batteries.

LOUISA EÉN & WILMA JÖNSSON

Department of Chemistry and Chemical Engineering
Chalmers University of Technology

Abstract

Plastics are among the most widely used materials today, and increasing the use of recycled plastics is a key strategy for reducing CO₂ emissions. This thesis investigates the impact of recycled polypropylene content and the bond line performance when joining components in the SPA3 battery for electric vehicles. The materials used in the study are virgin PP and the recycled plastics PIR30, PCR30, and PCR50. The abbreviation PIR stands for post-industrial recycled, and PCR stands for post-consumer recycled. The coupons are either untreated or treated with atmospheric plasma, plasma with precursor, or plasma followed by primer, respectively. After pretreatment, the plastic coupons were joined with a polyurethane-based two-component adhesive, and the strength of the joints was measured with single lap shear tests after curing and ageing. Surface analysis measurements of surface free energy, cleanliness, and surface roughness were also done to see the differences among the materials and how the surface properties changed after pretreatment. The result showed that the plasma pretreatment exclusively was superior among the pretreatments. Plasma-treated PIR30 and PCR30 received similar high strength as virgin PP, and plasma-treated PCR50 showed slightly lower strength. The results conclude that the recycled materials PIR30 and PCR30 are possible substitutes for virgin PP in the SPA3 battery package. PCR50 is also promising in this regard after optimisation and development when implementing high recycled polypropylene content.

Keywords: recycled polypropylene, polyurethane adhesive, surface-pretreatments, plasma, precursor, primer, SPA3 battery, electric vehicles.

Acknowledgements

This report would not have been possible without the support and guidance of our supervisor, Kerstin Wasmuth and co-supervisor Marcus Öhrby. We also want to thank Roy Johansson for always supporting us in the lab and during the LSS measurements. Thanks to the rest of the Surface treatment centre, especially Ghasseb Ibrahim, Simon Ljunggren, and Jesper Alm. Big thanks to the Battery Thermal & Joining team for welcoming us this semester. Thanks to Åsa Lundevall and RISE for their engagement in our project. We also would like to express our gratitude to the Material Centre, especially to Johan Schenström, for supporting us during our analyses. Lastly, we are sincerely thankful to Professor Magnus Skoglundh for great guidance during the project.

Louisa Eén, Wilma Jönsson, Gothenburg, May 2025

List of Acronyms

Below is the list of acronyms that have been used throughout this thesis listed in alphabetical order:

AF	Adhesion Failure
BLT	Bond Line Thickness
CF	Cohesion Failure
Coupon	The test-body, a rectangle with the dimensions 12 cm * 25 mm * 3 mm
DF	Delamination Failure
FTIR	Fourier Transform Infrared Spectroscopy
GLYMO	3-Glycidyoxypropyltrimethoxysilane
LSS	Lap Shear Strength
PCR30	Virgin PP with 30 % Post Consumer Recycled Polypropylene (with 30 % glass fiber)
PCR50	Virgin PP with 50 % Post Consumer Recycled Polypropylene (with 30 % glass fiber)
PIR30	Virgin PP with 30 % Post Industrial Recycled Polypropylene (with 30 % glass fiber)
PP	Virgin polypropylene (with 30 % glass fiber)
RFU	Relative Fluorescence Unit
SF	Substrate Failure

Contents

List of Acronyms	ix
List of Figures	xiii
List of Tables	xv
1 Introduction	1
1.1 Background	1
1.2 Aim and objectives	2
1.2.1 Limitations	2
2 Theory	3
2.1 Polypropylene	3
2.1.1 Fibre reinforced plastics	4
2.1.2 Processing methods of polypropylene in the automotive industry	4
2.1.3 Additives	5
2.1.4 Recycling procedures of polypropylene	6
2.1.5 Post-industrial recycled plastic and post-consumer recycled plastic	7
2.2 Pretreatments	8
2.2.1 Plasma	8
2.2.2 Plasma plus precursor	9
2.2.3 Primer	10
2.3 Surface analysis	10
2.3.1 Cleanliness	10
2.3.2 Surface free energy	10
2.3.3 Surface roughness	12
2.4 Adhesives	12
2.4.1 Polyurethane	13
2.5 Lap shear strength testing	13
3 Previous Studies	15
4 Methods	17
4.1 Pretreatments	17
4.1.1 Plasma	17
4.1.2 Plasma plus primer	18
4.1.3 Plasma plus precursor	18

4.2	Surface analysis	18
4.2.1	Cleanliness	18
4.2.2	Surface free energy	18
4.2.3	Surface roughness	19
4.3	Application of the adhesive	19
4.4	Curing and ageing procedures	20
4.4.1	Heat ageing	21
4.4.2	Tropical ageing	21
4.5	Lap shear strength testing	21
4.6	Study of cross-section of the coupons	21
5	Results and Discussion	23
5.1	Cleanliness	23
5.2	Surface free energy	24
5.3	Surface roughness	26
5.4	Failure of samples	27
5.5	Lap shear strength testing	28
5.5.1	PP	28
5.5.2	PIR30	30
5.5.3	PCR30	32
5.5.4	PCR50	34
5.5.5	Comparison of the materials with plasma treatment	36
5.6	Study of cross-section of the coupons	38
6	Conclusion	41
7	Future Outlooks	43
	Bibliography	45
A	Appendix 1	I

List of Figures

2.1	An illustration of how a thermoplastic behaves upon heating.	4
2.2	A simplified illustration of the SPA3 battery package including the cooling plate and cover lid, end plates, battery cells, and busbar carriers.	5
2.3	Overview of the injection moulding process, adapted from [18].	5
2.4	An illustration of the plasma instrument with the special jet head with an inlet for the precursor, adapted from [28].	9
2.5	The chemical structure of 3-Glycidoxypropyltrimethoxysilane (GLYMO), adapted from [30].	9
2.6	Surface forces acting when a liquid drop is dispersed on a surface.	11
2.7	An illustration showing two adherends connected by adhesive (in black), with the joint being the overlapping area where the two adherends are bonded together.	12
2.8	An illustration of how a thermoset polymer behaves upon heating.	13
2.9	An illustration of an LSS test where the adherends are joined together by the adhesive (in black) and a force (F) is applied in one of the ends.	14
2.10	Illustrations of four different failure modes gained from the Volvo standard. The adherends are the plastic substrate, and the adhesive is seen in black.	14
4.1	A photograph of the Openair-Plasma® with a rotational jet head during pre-treatment.	17
4.2	Scheme of the adhesive being applied on the coupons.	20
5.1	The average values of the parameters R_a and R_z for each material without pre-treatment. The average and the standard error are based on five measurements on each plastic. R_a is the roughness average and R_z is the mean roughness depth.	27
5.2	The averages of lap shear strength (in %) for all pretreatments of PP. The percentages are calculated based on the highest series average strength within the PP material. The average within each series is calculated based on five samples. The abbreviation <i>In</i> stands for initial (no ageing), <i>H</i> for heat ageing, and <i>T</i> for tropical ageing.	29
5.3	Failure modes for all PP samples. SF is substrate failure, AF is adhesion failure, and DF is delamination failure. SF/AF is a combination of SF and AF happening at the same time.	30

5.4	The averages of lap shear strength (in %) for all pretreatments of PIR30. The percentages are calculated based on the highest series average strength within the PIR30 material. The average within each series is calculated based on five samples, except for plasma + precursor In and H, where the average is based on four samples. The abbreviation <i>In</i> stands for initial (no ageing), <i>H</i> for heat ageing, and <i>T</i> for tropical ageing.	31
5.5	Failure modes for all PIR30 samples. SF is substrate failure, AF is adhesion failure, and DF is delamination failure. Note that plasma + precursor In and H are based on four samples in each series instead of five.	32
5.6	The averages of lap shear strength (in %) for all pretreatments of PCR30. The percentages are calculated based on the highest series average strength within the PCR30 material. The average within each series is calculated based on five samples, except for plasma + precursor T, where the average is based on four samples. The abbreviation <i>In</i> stands for initial (no ageing), <i>H</i> for heat ageing, and <i>T</i> for tropical ageing.	33
5.7	Failure modes for all PCR30 samples. SF is substrate failure, AF is adhesion failure, and DF is delamination failure. SF/AF and SF/DF combinations of failure modes that happen at the same time. Note that plasma + precursor T is based on four samples in the series instead of five.	34
5.8	The averages of lap shear strength (in %) for all pretreatments of PCR50. The percentages are calculated based on the highest series average strength within the PCR50 material. The average within each series is calculated based on five samples. The abbreviation <i>In</i> stands for initial (no ageing), <i>H</i> for heat ageing, and <i>T</i> for tropical ageing.	35
5.9	Failure modes for all PCR50 samples. SF is substrate failure, AF is adhesion failure, and DF is delamination failure. DF/AF is a combination of DF and AF that is happening at the same time.	36
5.10	The averages of lap shear strength (in %) for the plasma-pretreatments of PP, PIR30, PCR30, and PCR50. The percentages are calculated based on the highest average strength of all plasma series. The average within each series is calculated from five samples. The abbreviation <i>In</i> stands for initial (no ageing), <i>H</i> for heat ageing, and <i>T</i> for tropical ageing.	37
5.11	The failure modes of all the plasma-treated samples. SF is substrate failure, AF is adhesion failure, and DF is delamination failure. SF/AF is a combination of SF and AF happening at the same time.	37
5.12	Microscopic pictures of the cross sections. The pictures on the left were captured from above and the pictures on the right were taken from the side to provide different views of the surface structure.	39
5.13	The result from the CT scan of PP to the left and PIR30 to the right in each figure.	40
A.1	Pictures of the different failure modes from all the series of PP.	I
A.2	Pictures of the different failure modes from all the series of PIR30.	II
A.3	Pictures of the different failure modes from all the series of PCR30.	III
A.4	Pictures of the different failure modes from all the series of PCR50.	IV

List of Tables

5.1	The results from the cleanliness measurements representing the RFU values of the different materials before and after the specific pretreatments.	24
5.2	The results from the surface free energy measurements of all materials with their specific pretreatment. The table presents the measured contact angle (of water), the total SFE (γ_{tot}), the dispersive contribution to the SFE (γ_D) and the polar contribution to the SFE (γ_P), respectively. They are all presented as average values calculated from three measurements made on each sample surface. . . .	25

1

Introduction

Global warming poses a significant threat to the future, with CO₂ emissions established as a primary contributor to rising global temperatures [2]. In the past year, the global average temperature exceeded 1.5 °C above the pre-industrial levels, the Paris Agreement's established threshold. This contributes to the occurrence of extreme events, such as heat waves, wildfires, melting polar ice caps, and flooding. Companies need to explore and evaluate their material usage to drive sustainability and decrease their carbon footprint.

Plastics are widely used today in a broad variety of fields, everything from food packaging to construction, healthcare, and textiles [3]. It is a very versatile material with low production cost and is today one of the most widely used materials. According to the European Environment Agency [3], global consumption of plastics is increasing rapidly, but only 9 % of the plastic ever produced has been recycled, and 12 % has been incinerated. The production of virgin plastic contributes to climate change, where the annual emissions related to the production of plastic in the EU are around 13.4 million tonnes of CO₂, which is roughly 20 % of the chemical industry's emissions in the EU. Volvo Cars has set several goals in this regard, including achieving climate-neutral production by 2025 [4]. In 2018, the engine factory in Skövde was their first climate-neutral facility.

To reduce pollution and the release of greenhouse gases, efforts can be made to accelerate the transition to a circular and resource-efficient plastics economy. One step in the right direction is to use recycled plastic instead of virgin plastic.

1.1 Background

Volvo Cars has several environmental goals for the upcoming years. The company announced in June 2018 that the plastic material in all new Volvo models will contain at least 25 % recycled material by the year of 2025 as a part of the sustainability work [4]. By the year 2030, the goal is to have 35 % recycled material in all new cars, and that all material manufactured will be reused or recycled [5]. Furthermore, by the year of 2040, Volvo Cars aims to be a circular business, meaning that waste and pollution will be down to zero and new material intake will be reduced. Instead, reused and recycled material will be the primary material resource.

There are a lot of plastic components in the new SPA3 battery package of electric vehicles. The plastic used today is virgin polypropylene (PP) with 30 % glass fibres in the matrix. Recycled plastic can come from either consumers, which is called *post-consumer recycled (PCR)*, or from the industry, which is referred to as *post-industry recycled (PIR)*. Plastic coupons made of polypropylene with 30 % glass fibre will be used in the thesis work. Three materials out of

four contain a certain percentage of recycled plastic; 30 % PIR, 30 % PCR and 50 % PCR. The battery components are partly attached by using adhesives which has to adhere properly to the materials to guarantee the quality of the joint. How well the adhesives adhere to a material of partly recycled plastic is therefore of interest, and its behaviour is called bond line performance.

1.2 Aim and objectives

This study aims to examine the adhesion when joining recycled polypropylene and to analyse the mechanical and physical properties of the adhesive bond line in comparison to virgin polypropylene. It also includes different pretreatments and how they affect the adhesion of the different plastic surfaces.

The objectives for the thesis are to investigate if there are any complications with the adhesion to recycled polypropylene and its possibilities to be used instead of virgin polypropylene. Before adhesion, the plastics will be pretreated with either plasma, plasma combined with precursor, or plasma followed by primer to ensure a stronger joining. References without any pretreatment will also be made to determine the effects of the pretreatments. To investigate the differences between virgin and recycled polypropylene, several surface analysis methods will be used. These are cleanliness, surface roughness, and contact angle measurements. Lap shear strength (LSS) test will then be performed to measure the strength of the adhesion and to measure the mechanical and physical properties of the adhesive bond line.

1.2.1 Limitations

One limitation of the project is that all plastic coupons made of the same material are expected to be identical if they originate from the same production batch. Therefore, surface analysis of all coupons before pretreatment will not be performed and are therefore excluded from this study.

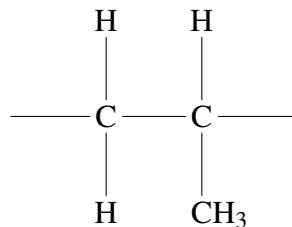
Another limitation is to exclude the investigation of the precise content of the recycled plastics. The recycled polypropylene used in this study is categorised as either PIR (post-industrial recycled) or PCR (post-consumer recycled), with unspecified filler and additive content by the producer.

2

Theory

2.1 Polypropylene

Polypropylene is a petrochemical product catalytically synthesized from propylene ($H_2C = CHCH_3$) through addition polymerization with the stereospecific *Ziegler-Natta catalyst* [6]. A stereospecific catalyst can direct a reaction and produce a product with specific stereoisomerism [7], where Ziegler-Natta catalysis has been considered as the best catalytic cycle to produce isotactic polypropylene [8]. Isotactic polypropylene has a higher degree of crystallinity than syndiotactic or atactic polypropylene, resulting in higher strength and stiffness. It is also considered a semi-crystalline polymer consisting of both crystalline and amorphous phases ordered in an intricate network [9]. Ziegler-Natta catalysts can be made of different combinations of organometallic compounds with metals from group one, two, or three in the periodic table, combined with halides or esters of transition metals from group four to eight [10]. The monomer of polypropylene is shown below [11], where the tacticity depends on the orientation of the CH_3 substituent at the chiral center [12].



In addition polymerisation, high energy radiation is applied together with an initiator or catalyst to connect the propylene monomers and build long chains of polypropylene [11]. PP is a polymer built on carbon and hydrogen atoms, which gives it a hydrophobic nature and a low surface energy. PP is a thermoplastic, which means that it softens upon heating and can then be shaped and formed before solidifying [13]. The structure of a thermoplastic is seen in Figure 2.1 where the polymer chains are straightened and untangled during heating.

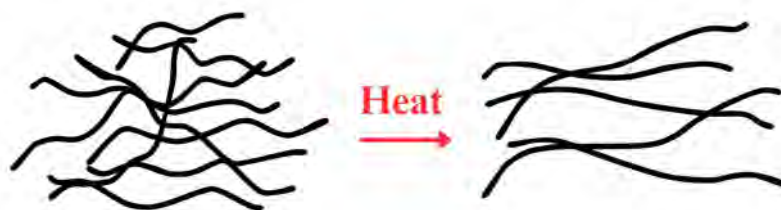


Figure 2.1: An illustration of how a thermoplastic behaves upon heating.

Thermoplastics can go through several cycles of heating and cooling without drastic damage, which allows for reprocessing and recycling of PP [13]. It is the lightest type of plastic and the most widely used among thermoplastics because of its affordability and flexibility [11]. Because of its crystalline parts, it also shows a high level of stiffness and a high melting point, but the properties of PP can vary depending on process conditions, copolymer components, and molecular weight distribution. Because of its great physical and mechanical properties, PP can be used in a wide variety of fields, where the automotive industry is one of them. The low weight of PP makes it an interesting plastic for the car companies that want to reduce the overall weight of the cars. It also has properties such as low water adsorption and good electrical resistance, which is advantageous for the battery of electric vehicles. PP is also suitable for reinforcing and filling to further modify the material for different applications.

2.1.1 Fibre reinforced plastics

Plastics can be reinforced by adding fibres to the polymer matrix, and this is called fibre-reinforced plastics and is a type of composite material [14]. The reinforced plastic obtains a combination of the components' properties. Fibres are strong and stiff in relation to their weight, which is beneficial if you want a strong and lightweight material. Therefore, the fibres make the plastic material stronger and reduce the risk of creeping. Additionally, designing, producing, and repairing reinforced plastics is relatively simple.

A common fibre to use is glass fibre, which is made of silicon dioxide (SiO_2) [14]. Glass fibres are commonly used in the automotive industry because of their low weight and cost combined with high durability and strength. However, the glass fibres exhibit poorer wettability than the organic polymer matrix and may decrease the wettability of the composite. The fibre versus polymer ratio is important to consider, and 30-60 vol% is generally practised for glass fibre reinforcement. A consequence of too high fibre content is structural quality problems.

2.1.2 Processing methods of polypropylene in the automotive industry

The plastic components inside the electric vehicle battery SPA3 that this study will focus on are called busbar carriers and end plates, marked in red in Figure 2.2. The busbar carriers are a part of the cell contact system (CCS) that is responsible for the connection between the individual battery cells within the battery module [15]. The busbar carriers hold the busbars in place and provide thermal and electrical insulation to prevent overheating and short circuits. This is due to the excellent physical and mechanical properties of polypropylene mentioned before [11]. They also ensure that the busbars do not expand during heating. The end plates provide longitudinal

support and stabilize the battery pack, but also provide insulation properties similar to the busbar carriers [16].

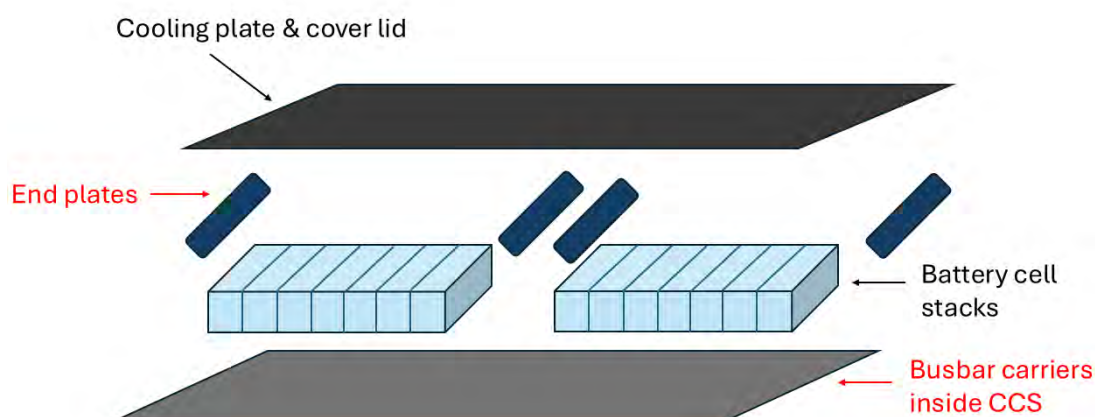


Figure 2.2: A simplified illustration of the SPA3 battery package including the cooling plate and cover lid, end plates, battery cells, and busbar carriers.

The busbar carriers and end plates are today made of PP with 30 % reinforced glass fibres and are both produced through a technique called injection moulding. In the process, plastic granulates are melted and injected into a mould which is designed for the specific part that is being moulded [17]. The molten plastic will fill the cavities of the mould, where it is held under pressure until solidified. The mould is then opened and released from the product.

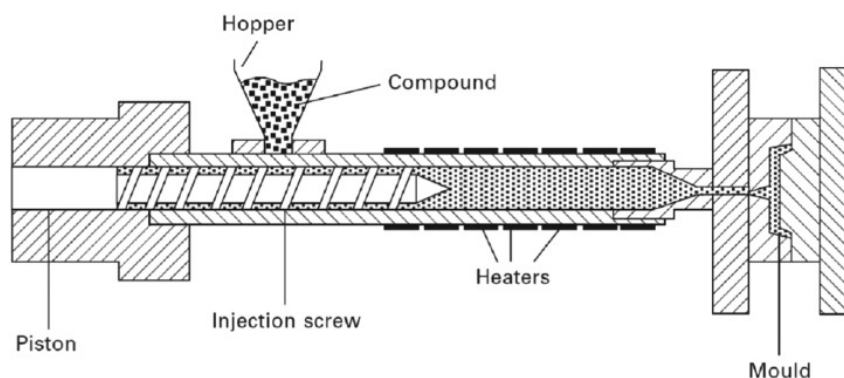


Figure 2.3: Overview of the injection moulding process, adapted from [18].

2.1.3 Additives

To receive the desired properties of the plastic material, additives are commonly added [19]. Additives are substances that affect the material during processing or the final product. The additives are, for example, UV-resistant agents, plasticizers, flame retardants, and other compounds with special physical and mechanical properties. The additives can be added as a solid or fluid to the plastic melt or onto the surface of the final product. A common issue during the in-

jection moulding process is that the plastic melt sticks to the mould, which is problematic when the product should be removed [20]. The attachment of the plastic melt to the mould occurs due to intermolecular forces arising between the plastic and the metallic mould. Furthermore, the high temperatures generated from friction against the walls of processing machines cause mechanical sticking. In order to solve these sticking problems, polished moulds without any sharp edges are preferred [20]. It can also be necessary to use release agents inside the mould, which can increase the production capacity for an injection moulding process. Common release agents used are silicones, waxes, and soaps, which can be used in various formulations such as powders, solutions, films, jellies, or oils.

Another form of release agents is internal release agents that are added to the polymer resin before processing [21]. These substances are typically a mix of waxes and esters, zinc and calcium stearates, or compounds of silicon and fluorocarbon. The exact mechanism by which the internal release agents work is not clearly understood. However, theories try to explain the mechanism. One explanation that the author Karbhari [21] raises is that the metallic stearates migrate to the surface during curing and form a thin fatty monolayer between the polymer object and the mould. Another suggestion is that the release agent is soluble in the polymer melt but becomes insoluble when the melt cures and is therefore ejected to the surface and forms a molecular separation layer.

2.1.4 Recycling procedures of polypropylene

Polypropylene is one of the most used commodity plastics and is used in various products, both single-use and long-lasting products [22]. It takes 20-30 years for polypropylene to completely decompose in landfills. This persistence is problematic due to the presence of additives, such as stabilizers, colourants, and plasticizers, which may contain hazardous elements like cadmium and lead and therefore pose a significant risk of environmental contamination. Furthermore, burning of thermoplastics can emit hazardous substances, contributing to air pollution. To avoid these consequences, there are three ways to recycle plastic products; primary recycling, mechanical recycling, and chemical recycling [23]. Before any recycling process can take place, the material has to be collected, cleaned, and sorted.

Primary recycling is to reuse the product in its original form [23]. This is the cheapest and simplest way of recycling. However, it is limited by the purposed application of the product and the number of reused cycles possible.

Mechanical and chemical recycling utilise the polymeric material in a new product [23]. Mechanical recycling treats the plastic by physical reprocessing in order to separate the material from contaminants and then form granulates by cutting and shredding the plastic. Thermoplastic granulate will be reprocessed by melting and extrusion to form new products. Virgin material can be added to the plastic melt to obtain or maintain a certain material quality. Thermoset granulates, on the other hand, can be used as fillers, for example in cement kilns, but are not suitable for further processing as they can not be remelted and reformed. To receive a usable and functional material, the plastic that will be mechanically recycled needs to be homogenous and relatively clean.

In chemical recycling, the chemical structure of the polymer in plastic will be changed [23]. In the process, the polymers will be depolymerised into smaller molecules, into oligomers or monomers. These molecules are then used as the feedstock material for re-polymerisation to the original polymer or production of new polymeric materials. Because of the re-polymerisation of the plastic, the recycled material turns into a valuable resource of high quality. There exist different routes and mechanisms for chemically recycled plastic, and the chosen way is optimised for the polymer in question. Polypropylene is a vinyl polymer, and due to the random scission of the C-C bonds, it cannot be chemically broken down into its monomers by adding simple chemicals. The two primary chemical recycling methods for polypropylene are therefore thermal degradation and catalytic degradation. Thermal degradation requires high temperatures, 500 up to 900 °C, and a variety of products can be produced by this process. Catalytic degradation involves different types of heterogeneous catalysts, for example, zeolites, and can operate at lower temperatures. Specific catalysts can produce a narrower distribution of hydrocarbon products.

A challenge with recycled plastic is to maintain the quality of the second-life material [24]. To do so, additives can be added to the recycled plastic. One of the most commonly used additives for homogenous polymeric materials is re-stabilisers to slow down or avoid the degradation of the polymers. Another method is the addition of modifiers and fillers to improve the quality without affecting the overall cost. When recycling heterogeneous polymers, the main challenge is the mixture of chemical structures, and the material will receive poor quality if the polymers are incompatible with each other. Therefore, chemical compatibility is an important aspect during the recycling process, and additives called compatibilisers are used.

2.1.5 Post-industrial recycled plastic and post-consumer recycled plastic

Recycled plastic can be divided into two groups depending on its origin, as mentioned in the background, post industrial recycled plastic (PIR) or post consumer recycled plastic (PCR). PIR plastic originates from production in the industry and can be seen as a by-product rather than waste because of its high value for other areas of use [25]. The PIR plastic usually has a well-known composition and mostly consists of uncontaminated monomaterials. This results in less material loss and a final recycled material with higher quality compared to PCR plastic. However, this material inflow is limited by the virgin plastic production, and this cycle does not close the material life cycle since it is not a renewable resource.

Post-consumer recycled plastic consists of material from products that have been used on the market by consumers [25]. This results in a pre-process to collect and separate the material from impurities, which leads to material losses. The PCR material often ends up with lower quality than the PIR plastic because of the material mixture, pre-processes, and additives. PCR closes the material life cycle, on the other hand, because the material can be used many times after the product's end of life.

The study written by Schulte, Kampmann, and Galafton [25] investigated the environmental efficient circularity, climate change, and the impact reduction potential of PIR and PCR polypropylene [25]. According to the case study, the PCR had better results for the environmental efficiency and circularity. On the other hand, PCR had higher values for climate change impacts compared with PIR. In an ideal circulation loop, the study suggests that virgin

polypropylene can be recycled nine times. The study also showed that effective circularity of the polypropylene recycling loop directly increased with better collection, sorting, and higher volume of recycled material.

2.2 Pretreatments

Polyolefins, such as polypropylene, are built on carbon and hydrogen atoms, which gives them low surface energy and a hydrophobic nature due to the lack of functional groups. Polypropylene has, on the other hand, desirable characteristics such as low density, ease of processing, high thermal stability, high chemical resistance, and cost-effectiveness, making it interesting in various industries [26]. Surface activation of polypropylene is an important field to make the surface prone to painting, adhesion, or printing, among others. There are several ways to activate polypropylene surfaces in pretreatment steps, where this project aims to test plasma, plasma plus precursor, and plasma followed by primer on both virgin and recycled polypropylene.

2.2.1 Plasma

Plasma is referred to as the fourth state of matter among gas, liquid, and solid states [27]. The sun, galaxies, and stars in the universe are composed of plasma, and flames and lightning are partly made of plasma. Plasma is formed when energy in the form of heat is applied to a gas, and eventually, the gas becomes ionized as the molecules and atoms release electrons. In total, the plasma is a mixture of free electrons, radicals, ions, and fragments of excited molecules.

Plasma has high electrical conductivity because of its high unstable energy levels, making plasma highly chemically reactive [27]. Therefore, the plasma can easily react with different surfaces and change the surface structure. For example, a non-polar surface can become polar for a certain amount of time, and this can be used in many applications. The change in surface energy makes it possible for a hydrophobic surface to interact with a hydrophilic material. The plasma used in the project is generated from air, primarily consisting of oxygen and nitrogen. Due to the high energy of the plasma, oxygen and nitrogen ions interact with the plastic surface, leading to the formation of polar groups, which theoretically promotes surface wettability and adhesion [27]. See figure Figure 2.4 for an illustration of the plasma instrument.

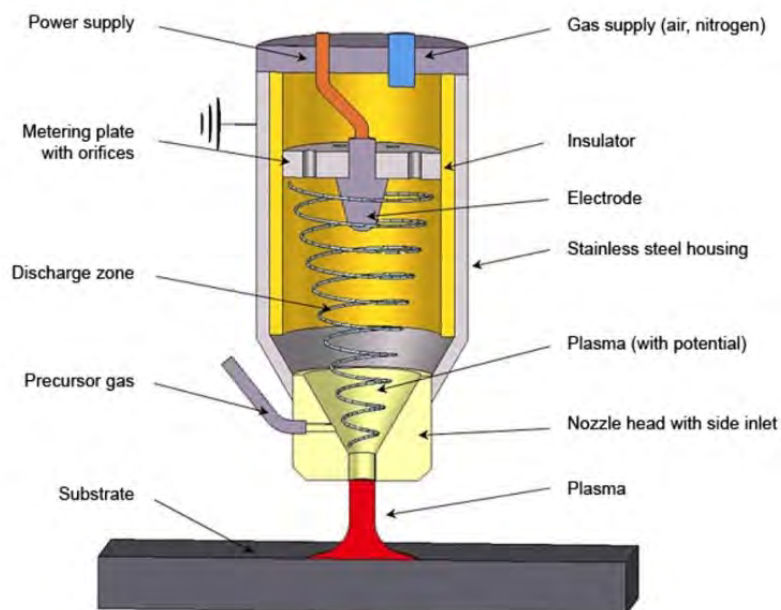


Figure 2.4: An illustration of the plasma instrument with the special jet head with an inlet for the precursor, adapted from [28].

2.2.2 Plasma plus precursor

A precursor can be added to the plasma treatment by adding a special jet head (nozzle head) [28], see Figure 2.4 for an illustration of the instrument. The precursor is in the liquid phase at room temperature and stored in a separate tank connected to the jet head. The precursor is vaporised and introduced directly to the plasma by a carrier gas, and when the precursor blends with the plasma, it becomes excited and very reactive. The mixture is then applied to the substrate, and the precursor creates a nano-coating. The precursor provides several sites for the adhesive to bind to, and may therefore theoretically improve the adhesion [29].

The precursor used in the experiment is 3-Glycidoxypropyltrimethoxysilane, or shortly GLYMO, which is a trifunctional epoxy-terminated organosilane, see chemical structure in Figure 2.5 [30].

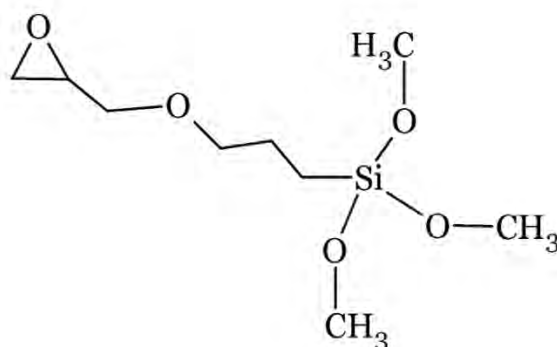


Figure 2.5: The chemical structure of 3-Glycidoxypropyltrimethoxysilane (GLYMO), adapted from [30].

GLYMO has been used in a wide range of surface modification applications and for different purposes, where improved adhesion is one of them [30]. The silane (-Si(OCH₃)₃) end of GLYMO will hydrolyse into silanol (-SiOH) groups, which covalently or hydrogen bond to the polar functional groups present on the PP surface from the plasma [31]. The reactive epoxy end of the molecule will covalently bind to the polyurethane adhesive, and GLYMO is considered an important coupling agent, improving the adhesion [30].

2.2.3 Primer

Another important pretreatment is the primer technique, which is useful in the automotive industry [32]. In this pretreatment, a small amount of polymer solution is applied, forming an adhesive layer. The primer and the polypropylene surface are connected through the interlocking of the polymer chains to the substrate, creating a stable interphase between the materials. To enhance the adhesion between the primer and the plastic surface, the PP coupons can be plasma pretreated before the primer is applied. The primer will then interact with the adhesive applied through intermolecular interactions of the polar functional groups of both the primer and the adhesion [32]. This technique will increase adhesion properties and improve the resistance to several external stresses.

2.3 Surface analysis

Surface analysis will be performed on all plastics before and after pretreatments to investigate structural differences on the surface.

2.3.1 Cleanliness

It is important to measure cleanliness before adhesion to detect unwanted contaminations and ensure product quality [33]. The CleanoSpector emits UV light onto the surface and measures the fluorescence from any organic contaminants present on the surface [34]. Cleanliness is measured in RFU, which stands for *Relative Fluorescence Unit*. If a surface contains a high amount of organic contaminants, the CleanoSpector will show a higher RFU value. So to have a clean surface, a low RFU value, or a low difference in RFU before and after pretreatment is preferable for better adhesion.

2.3.2 Surface free energy

Surface free energy (SFE) is the work needed to expand the unit area of a solid when separating two phases and is used to quantify the surface tension of solids [35]. This thermodynamic parameter cannot be measured directly due to the insufficient mobility of solid surfaces, but calculation approaches using contact angle measurements are sometimes preferred. Calculations of the SFE are based on Young's equation for ideal systems, which is seen in Equation 2.1.

$$\gamma_{SG} = \gamma_{SL} + \gamma_{LG} \cdot \cos(\theta) \quad (2.1)$$

The parameter γ_{ij} refers to the interfacial tension between the solid (S), liquid (L), and gas (G). ij is S, L, or G and θ is the contact angle at equilibrium [36]. All parameters are illustrated in Figure 2.6 below.

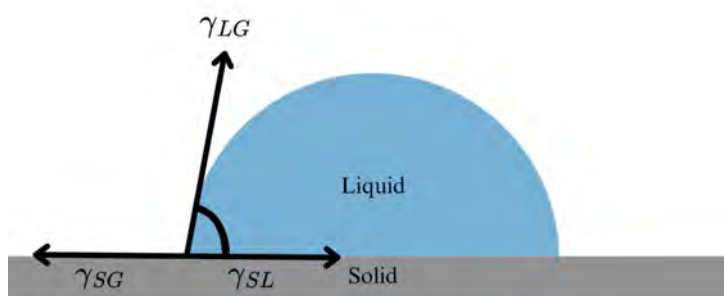


Figure 2.6: Surface forces acting when a liquid drop is dispersed on a surface.

Young's equation can then be reformulated to a form used for calculations, see Equation 2.2.

$$\gamma_S = \gamma_{SL} + \gamma_L \cdot \cos(\theta) \quad (2.2)$$

In this equation, the γ_S is the SFE of solids in vacuum, γ_{SL} is the interfacial tension between the solid and the liquid, γ_L is the measured SFE of the liquid, and θ is the measured contact angle when the liquid is dispersed onto the surface.

One method for determining the SFE is the Owens-Wendt-Rabel-Kaelble (OWRK) method, where the dispersion and polar components, γ_D and γ_P respectively, of the SFE are determined [36], see Equation 2.3. This method relies on the Bethelot hypothesis, which means that the interactions between molecules present in the surface layers of two substrates are equal to the geometric mean of intermolecular interactions within each substance. The polar component (γ_P) is a sum of polar, hydrogen, inductive, and acid-base interactions, whereas the dispersive component (γ_D) is a sum of the dispersion forces present.

$$\gamma_T = \gamma_D + \gamma_P \quad (2.3)$$

A lower contact angle (θ) results in a higher wettability, and the liquid droplet will spread more onto the surface. When dispersing a water droplet, low contact angles are signs of hydrophilic surfaces, but if the contact angle is 90° or higher, the surface is considered hydrophobic [37]. The wettability or the degree of wetting depends on the adhesive forces between molecules in the liquid and surface, and the cohesive forces of the droplet dispersed [37]. The adhesive forces favour the wetting, and cohesive forces work against wetting. The wettability of a liquid onto a surface can be related to surface energy with Equation 2.1 and Equation 2.2. Measuring the contact angle is crucial to determine if the pretreatments increase the total surface energy, especially the polar contribution, ensuring proper adhesion and effective wetting of the surface.

2.3.3 Surface roughness

Surface roughness is an important factor to consider when talking about adhesion. A rough surface generally has a higher surface area, meaning it increases the connected surface between the material and adhesive, hence increasing the overall adhesion [38]. However, for a surface that is extremely rough with numerous grooves, the opposite effect may be observed, as this can reduce the contact area between the surface and the adhesive. This has been observed in a study made by Encinas, Abenojar, and Martínez [39], discussed in chapter 3, where they concluded that the adhesive had trouble entering the grooves and valleys of the abraded polypropylene. Viscous adhesives may have problems of properly wetting highly rough surfaces, which generally decreases the adhesion.

Surface roughness aims to determine the quality of the surface's texture by measuring the deviation in the vertical direction when compared to ideal surfaces [40]. When the deviation is high, it indicates a highly structured surface and vice versa. Common parameters used when measuring surface roughness are R_a and R_z [41]. R_a is the arithmetic average of the roughness profile, representing the average height deviations from the nominal surface and reflecting the roughness height over a given length L [40]. R_z is the mean roughness depth and is an average of the five highest peaks and five lowest valleys over a specific sampling length L [41]. A surface with high roughness will exhibit high R_a and R_z values, whereas a smooth surface will have correspondingly lower values for these parameters.

2.4 Adhesives

Adhesives are used for adhesive bonding and connect two parts in the solid state, which are called the *adherends* [42], see Figure 2.7. Adhesives are capable of forming bonds between two adherends, and only a small amount is required relative to the total weight of the joined parts [43]. Another advantage of adhesives is their ability to transfer stress through the adhesive joint, distributing it more evenly over a larger area than mechanical fasteners like screws and bolts. As a result, adhesive bonds can create joints that are equally strong or even stronger than traditional assemblies while reducing both cost and weight.

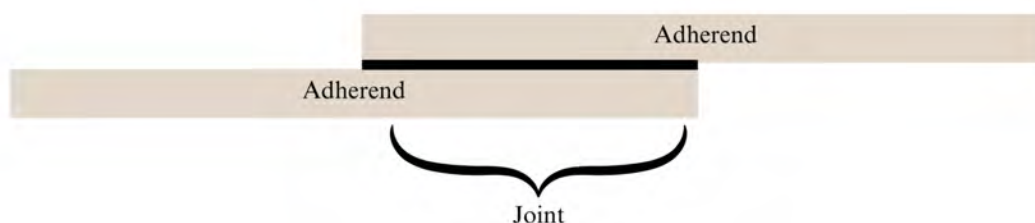


Figure 2.7: An illustration showing two adherends connected by adhesive (in black), with the joint being the overlapping area where the two adherends are bonded together.

Adhesive bonds can be classified as either structural or non-structural [43]. The structural adhesive bonds refer to the strong bonds where the adherends are capable of transmitting the stress when they are exposed to high strain. A structural bond is characterized by its ability to

withstand shear forces greater than 7 MPa while maintaining durability over time and resisting degradation caused by environmental factors such as heat and moisture. These types of adhesion bonds are ideal for joining in automotive applications. A non-structural bond is a relatively weak adhesion and its primary task is to hold lightweight materials in place [43]. These types of bonds are often referred to as "holding adhesives" and have applications such as tapes and packaging adhesives.

Adhesives can have many different properties, such as flexibility or rigidity, and weakness or strength [42]. To bond composite materials, such as plastics, adhesives always have to cure at either room or elevated temperatures.

2.4.1 Polyurethane

The adhesive used in this project is a two-component polyurethane adhesive, which is a thermoset polymer. Polyurethane adhesives are widely used in the automotive industry due to their resistance to petrol, oils, greases, and water [44]. A two-component product consists of two distinct substances that chemically react upon mixing. The two components, isocyanate and polyol, form the polyurethane when the isocyanate groups react with the alcohol groups [45]. After curing and hardening of a thermoset, the polymer chains are connected by chemical cross-links, which makes them rigid after solidification [13]. Due to this structure, thermosets retain their shape during heating and cannot be reshaped, see Figure 2.8 for an illustration of this.

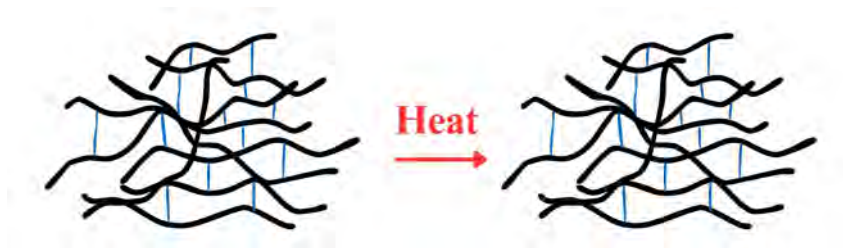


Figure 2.8: An illustration of how a thermoset polymer behaves upon heating.

Polyurethane is built on the urethane monomer, $(-\text{NH}-\text{CO}-\text{O}-)_n$, where the side groups give the polymer its polar behaviour in total [46]. The adhesive used in the project is a high-viscosity paste that will be applied as a bead and will not flow unless shear stress is applied.

2.5 Lap shear strength testing

Lap shear strength (LSS) is a common technique to measure the stress and failure in stress of the adhesive component [42]. The two adherends are partly joined together by adhesion, and after curing and ageing, the LSS test can take place. One side of each adherend is connected to the device, which then pulls them apart, illustrated in Figure 2.9. The force is measured until the joint fails, and the failure mode will be investigated.



Figure 2.9: An illustration of an LSS test where the adherends are joined together by the adhesive (in black) and a force (F) is applied in one of the ends.

There are several possible failure modes, and Figure 2.10 shows four different ones, including adhesion failure (AF), cohesion failure (CF), delamination failure (DF), and substrate failure (SF), respectively. These are gained from one of Volvo Cars' standards. Adhesion failure is when the joint fails between the adherend and the adhesive, whereas cohesion failure is when the joint fails within the adhesive. Delamination failure happens if a coating is applied, for example a primer, and releases from the surface. Substrate failure is when the substrate itself breaks. It is also possible to get a mixture of failures, for example, 50% AF and 50% CF.

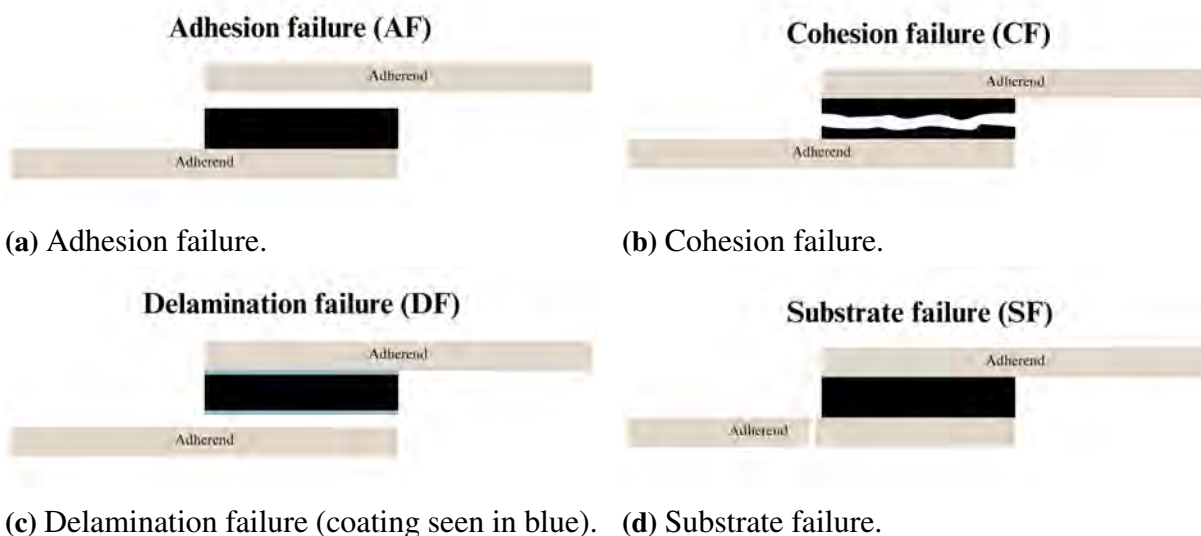


Figure 2.10: Illustrations of four different failure modes gained from the Volvo standard. The adherends are the plastic substrate, and the adhesive is seen in black.

3

Previous Studies

One previous study relevant for this project, made by Encinas, Abenojar, and Martínez [39], investigated different pretreatment methods for polypropylene with a one-component polyurethane-based adhesive. The study includes the following pretreatments: abrasion with emery paper of 80 grain size, a chemical primer and atmospheric pressure air plasma torch. Contact angle measurements were used to evaluate the wettability of the material, and the strength of the joints was measured using single lap shear strength tests.

The abraded PP showed a very small increase in surface energy (2 % compared to the untreated sample), and a small increase in shear strength compared to the untreated sample, which also showed a relatively low strength. According to the authors [39], this has to do with a combination of different factors such as low surface energy of the substrate and bad wetting of the adhesion due to difficulties filling grooves and valleys in the abraded polymeric material. However, the plasma treatment increased the surface energy of the PP more than two times compared to the untreated one and resulted in a six times higher shear strength during LSS testing. They further discussed that this increase in tensile strength was achieved because of an increase in the total and polar components of the surface energy and a result of the introduction of hydrophilic functional groups on the PP surface. When applying the chemical primer alone, the shear strength decreased a lot compared to the untreated sample, but in combinations with plasma treatment before and/or after the primer, the shear strength increased drastically. The authors could therefore conclude that the most successful pretreatment with the highest possible adhesion was the chemical primer with plasma treatment before and after applying the primer. Even though the primer was selected specifically for the adhesive, it was necessary to do plasma treatment to get proper adhesion between the PP and the primer without any peeling off. Encinas, Abenojar, and Martínez, [39], concluded that this result was probably a combination of the low surface energy of PP and the incompatibility of PP and the primer. They further discussed that the driving force of the adhesion of PP with polyurethane was based more on chemical interactions than physical interlocking gained during abrasion.

Another study made by Aurrekoetxea, Sarrionandia, Urrutibeascoa, *et al.* [47] investigated how the microstructure and mechanical properties of isotactic PP will be affected upon recycling. To do that, the PP was injection moulded several times to simulate the recycling procedure. The authors found that the melt viscosity reduced due to a decrease in the molecular weight after several injection moulding cycles. Aurrekoetxea, Sarrionandia, Urrutibeascoa, *et al.* [47] also concluded that recycled PP have a higher crystallisation rate, a higher degree of crystallinity and a higher equilibrium melting temperature than virgin PP. The recycling steps also increased the elastic modulus and yield stress for the PP, but decreased elongation at break and fracture

toughness. However, it is important to note that this study does not investigate recycled plastic directly, but rather examines how the properties of virgin PP are affected by multiple injection moulding cycles.

One study performed by Sanguanwong, Nikzad, Sbarski, *et al.* [48] investigated the use of a blend of PCR and PIR plastic in non-visual and non-structural components for the interior of vehicles in the automotive industry. The PIR plastic was a composite composed of ethylene vinyl acetate with 75 volume% ceramic powder originating from the plastic manufacturing industry. The PCR material originated from the collection of printer cartridges, which was based on olefins and non-olefins. Analysis with Fourier Transform Infrared Spectroscopy (FTIR) showed that the PCR plastic consisted of various thermoplastics, including polypropylene. The PCR plastic was decontaminated before it was shredded into smaller pieces, pellets, and blended together with PIR plastic pellets. The pellets from both materials were then processed by two methods, compression moulding and injection moulding.

Successful prototypes were manufactured in a pilot plant [48]. Injection moulding was seen to be a better alternative than compression moulding as moulding techniques, because of higher consistency of the produced specimens and higher flexural and tensile strength. The study reveals that the recycled material reduces the material cost by 40 %. Additionally, it turns out to have higher stiffness and the same tensile strength as virgin polymers. Thermogravimetric and rheological analyses confirm that the recovered polymer waste maintained thermal stability and shear-thinning behaviour. This indicates its suitability as a feedstock for conventional plastic processing methods.

4

Methods

4.1 Pretreatments

Several pretreatments were done prior to application of the adhesive, these pretreatments and their settings are presented in this section.

4.1.1 Plasma

The plasma treatment was performed by the Openair-Plasma® system from Plasmamatreat. The rotating jet head will give the plasma its wide beam seen in Figure 4.1. The instrument model was RD1004, and the generator model was FG5001, which has a power of 300-800 W when generating the plasma. The plasma instrument had a movement speed of 150 mm/s, and the plasma generator had an airflow set of 47 l/min. The jet head article number was 22826 with a diameter of 22 mm (treatment width), an opening width of 4 mm, and it rotated at a speed of 2700 rpm. The distance between the substrate and the jet head was approximately 13.5 mm, depending on the condition of the fixtures. The coupons were treated in groups of ten in the fixture.

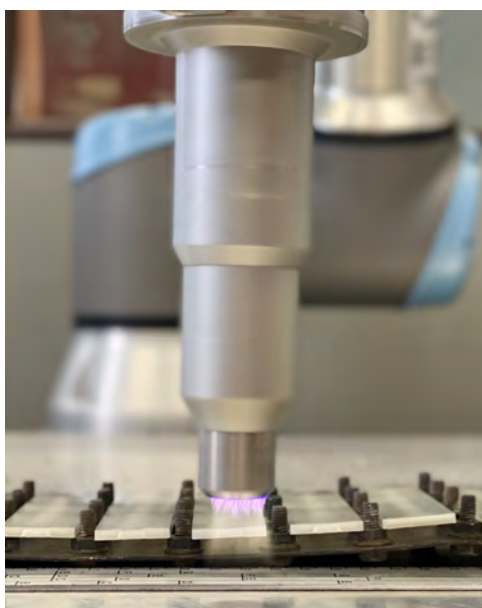


Figure 4.1: A photograph of the Openair-Plasma® with a rotational jet head during pretreatment.

4.1.2 Plasma plus primer

The adhesion-promoting primer used in the project was a black chemical primer based on polyisocyanates suitable for plastics and painted substrates. The isocyanate groups bind to the polyol molecules in the polyurethane adhesive. Firstly, the coupons were treated with plasma to enhance the adhesion of the primer to the PP coupons. Then, the primer was applied with an applicator in a thin layer and dried for five minutes before the adhesive was applied on the primed surface. The plasma parameters used are the same as above, subsection 4.1.1.

4.1.3 Plasma plus precursor

This pretreatment was performed at RISE in Mölndal using the Openair-Plasma® system from Plasmamatreat in the model PFW10PD with the generator model FG5001. The process gas was air, and the precursor used in the experiment was 3-Glycidoxypropyltrimethoxysilane, or shortly GLYMO. Firstly, the plastic surfaces were activated by the plasma only, and then the procedure was repeated, including the precursor GLYMO, which was applied continuously together in a mixture with the plasma.

The running speed was 100 mm/s, the distance from the jet head to the surface was 12 mm, and the effect of the plasma treatment was 300-600 W. The jet head used was non-rotating, compared to the plasma jet head in subsection 4.1.1, and had the article number 10147. Instead, the plasma was applied as a flame in sections with a width of 4 mm distance. The process gas flow was set to 35 l/min, the precursor flow was 5 g/h, and the precursor carrier gas (air) flow was 5 l/min.

4.2 Surface analysis

The methods of surface analysis done in the project are described in this section.

4.2.1 Cleanliness

Surface cleanliness was assessed using the CleanoSpector handheld measuring device from SITA. The device was applied directly to the test surface for three seconds while performing a scan. For each sample, six RFU readings were taken, and the average value was then calculated and used for further analysis. These readings were performed on one coupon of each material before and after the specific pretreatment.

4.2.2 Surface free energy

The SFE of the surfaces before and after the pretreatments was done using the KRÜSS ADVANCE Mobile Surface Analyzer. It analysed the wettability by dispersing a droplet of distilled water and diiodomethane (methylene iodide), respectively, with known surface tensions and contributions of the SFE. Firstly, 1 μ l of distilled water was dispersed onto the surface, and the polar contact angle was measured after 5 s to ensure equilibrium of the droplet spreading. After that, 1 μ l of diiodomethane was released, and the dispersed contact angle was measured

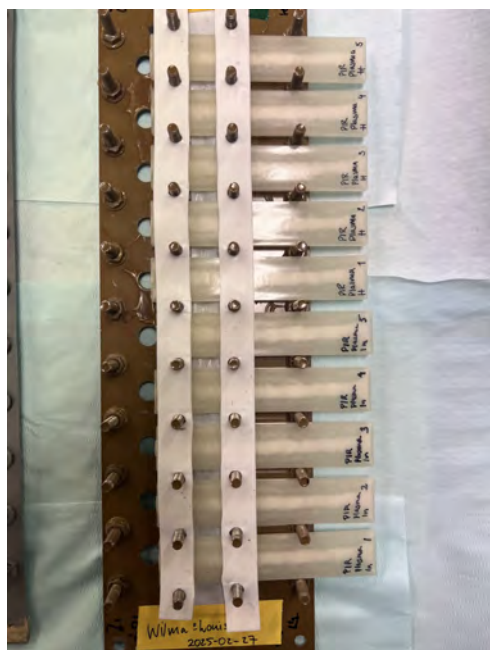
with the same 5 s delay. Three replicates of each sample were done, and the ADVANCE® programme calculated mean values for all contact angles, the total SFEs, and the polar and disperse contributions to the SFE according to the OWRK model described in subsection 2.3.2.

4.2.3 Surface roughness

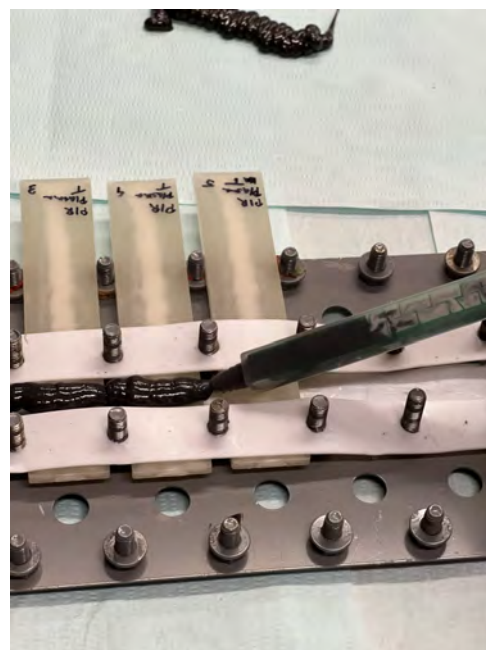
Surface roughness measurements were performed to investigate the differences among the plastic materials and assess whether these differences may explain the adhesion results. For this, an instrument from Mahr called MarSurf GD 120 was used. The model of the used probe head was MFW 250 B 6852501, and the model of the probe arm was 6852404 20200. The diamond tip on the probe arm moved in a straight line across the surface, and measurements of R_a and R_z were made. The measurements were performed on five coupons per material without any pretreatments, and the average R_a and R_z values were calculated accordingly.

4.3 Application of the adhesive

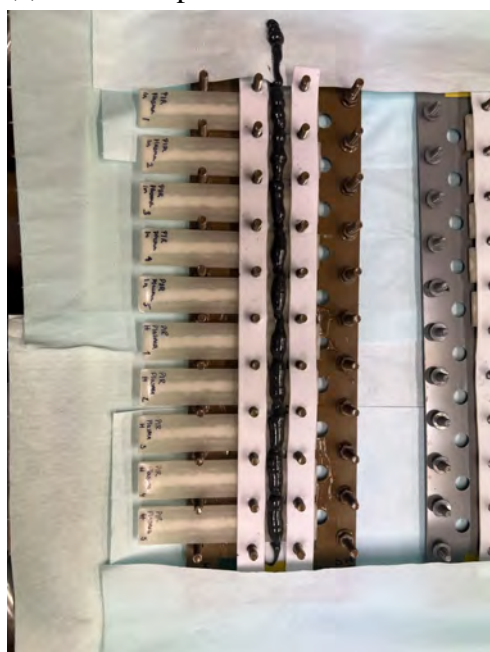
White strips made of polytetrafluoreten (PTFE) were placed on the coupons in the fixture because the adhesive does not adhere to PTFE, see Figure 4.2a. The strips were 1 mm thick and ensured that the bond line thickness (BLT), the thickness of the adhesive, became 1 mm. The bond area was approximately 12.5 · 25 mm on each coupon, but was measured exactly after each LSS test. To apply the adhesive, an applicator driven by pressured air was used. One tube of each adhesive component was attached to the applicator and their content was mixed by a mixing nozzle, see Figure 4.2b. When the adhesive had been applied, coupons with no adhesive were placed over the ones that had just been treated, and screw-nuts were fastened to ensure that the coupons remain in place and to achieve a BLT of 1 mm, see Figure 4.2d.



(a) Clean coupons in the fixture.



(b) Adhesive being applied.



(c) Coupons with adhesive.



(d) Attached coupons.

Figure 4.2: Scheme of the adhesive being applied on the coupons.

4.4 Curing and ageing procedures

After application of the adhesive, the samples were cured for one week in a room with the constant climate of 23 °C with 50 % humidity. Additionally, some samples were aged in a heated climate and some in a tropical climate, respectively.

4.4.1 Heat ageing

Heat Ageing was performed using an oven at 65 °C where one third of the samples were placed for three weeks. After this, the samples were placed at room temperature to cool for about 1-3 hours before the LSS test could take place.

4.4.2 Tropical ageing

Another third of the joined coupons were placed for two weeks in a tropical cabinet with 100 % relative humidity and elevated controlled cycles of temperatures between 23-40 °C. This Ageing procedure was done to investigate the moisture resistance of the jointed material.

4.5 Lap shear strength testing

The lap shear strength testing was performed on the jointed samples using a Zwick Z050 tensile tester with a test speed of 10 mm/min and a pre-load of 5 N. The test temperature of 23 °C was controlled and entered into the settings for each sample series. The lap strength was then calculated with Equation 4.1, which is based on the failing load and the manually measured joint area for each sample.

$$S = \frac{F_{max}}{A} \quad (4.1)$$

S is the lap shear strength at break, F_{max} is the failing load and A is the measured joint area [42].

4.6 Study of cross-section of the coupons

A microscopic analysis was performed to examine the distribution and orientation of the glass fibres within the material. This investigation was prompted by the appearance of the test coupons, particularly the presence of a distinct white region at the centre. To study the substrate's cross-section, a stereo microscope of the model LEICA M205 C was used. Samples with substrate failure (SF) were selected to enable a clearer view of the internal structure of the plastic bulk material.

To complement the microscopic study, a CT scan of PP and PIR30 was performed. These plastics were selected due to their significant differences in appearance, which made them ideal for a comparative analysis. The instrument used was FF35 CT, where an X-ray source emits beams towards the rotating sample, in this case, two plastic coupons. A detector opposite to the X-ray source will collect the X-rays. Several pictures were captured of the object from different angles, and they were combined to create a 3D model. This model was then analysed with the software VGSTUDIO MAX.

5

Results and Discussion

5.1 Cleanliness

The RFU value for all untreated, plasma-treated, and materials pretreated with plasma plus precursor were extremely high, with values exceeding 3000, see Table 5.1. This generally means that the surfaces have a lot of organic contaminants or components present on the surface. Since polypropylene has building blocks of carbon and hydrogen, the material itself is completely organic. The CleanoSpector will emit UV light and measure the fluorescence scattered from any organic compounds, reaching several layers into the material. Because of this, a polymeric material will always give high values of the RFU, even though the surface is cleaned with plasma. A high RFU value for organic materials is therefore expected, but it could be of interest to investigate changes in the RFU value when applying different pretreatments to the coupons. In Table 5.1, it is seen that the RFU values have decreased to some extent for the untreated samples after the plasma treatment, but the difference is very small. This decrease may be a result of fewer organic contaminants on the surface, suggesting that the plasma treatment improves the surface cleanliness. The addition of reactive polar fractions during plasma treatment may also affect the observed result.

The high RFU values for the plasma plus precursor treated coupons are also expected since the GLYMO molecule is an organic compound. Additionally, the GLYMO molecules are applied in a thin monolayer and the UV light will emit further down, reaching the polymer bulk in the coupons.

One exception to the high RFU values was the primer-coated samples. The primer is a black liquid that creates a dark layer when applied to the coupons. RFU values of the materials with the primer applied ranged from 75.1 to 214.1. This is a significant difference compared to the high values of the other samples. This decrease can be due to the colour of the primer, because a black surface generally absorbs more of the light spectrum and therefore re-emits less, leading to a lower RFU value. This hypothesis was tested by measuring the cleanliness of a black polypropylene piece, which received an RFU value of 30.6. The decrease seen for the primed samples can also be due to a cleaner surface with fewer contaminants. However, the primer-treated coupons still receive generally high RFU values, indicating organic substances, which is expected since the primer is polymer-based as well.

The overall impression from the cleanliness measurements is that it is not optimal to use a CleanoSpector when investigating organic polymeric materials. All materials and pretreatments show extremely high RFU values, even the smallest value of 75.1 for PP plasma plus primer is a high value in this context.

Table 5.1: The results from the cleanliness measurements representing the RFU values of the different materials before and after the specific pretreatments.

Material	Pretreatment	RFU
PP	Untreated	> 3014
	Plasma	> 3002
	Plasma + precursor	> 3034
	Plasma + primer	75.1
PIR30	Untreated	> 3022
	Plasma	> 3007
	Plasma + precursor	> 3002
	Plasma + primer	163.9
PCR30	Untreated	> 3029
	Plasma	> 3011
	Plasma + precursor	> 3023
	Plasma + primer	214.1
PCR50	Untreated	> 3028
	Plasma	> 3023
	Plasma + precursor	> 3035
	Plasma + primer	175.8

5.2 Surface free energy

The results from the SFE measurements are seen in Table 5.2, including the contact angle of water, total SFE (γ_{tot}), as well as the dispersive (γ_D) and polar distributions (γ_P) to the SFE. They are all average values calculated from three measurements made on each sample.

Table 5.2: The results from the surface free energy measurements of all materials with their specific pretreatment. The table presents the measured contact angle (of water), the total SFE (γ_{tot}), the dispersive contribution to the SFE (γ_D) and the polar contribution to the SFE (γ_P), respectively. They are all presented as average values calculated from three measurements made on each sample surface.

Material	Pretreatment	Contact angle (°)	γ_{tot} (mN/m)	γ_D (mN/m)	γ_P (mN/m)
PP	Untreated	104 ± 2.4	31.7 ± 0.8	31.7 ± 0.7	0.04 ± 0.08
	Plasma	60.2 ± 0.7	52.6 ± 0.7	40.6 ± 0.3	12.0 ± 0.4
	Plasma + precursor	31.3 ± 2.0	68.6 ± 2.3	40.7 ± 1.2	27.9 ± 1.2
	Plasma + primer	93.6 ± 0.4	39.1 ± 1.2	38.6 ± 1.1	0.52 ± 0.1
PIR30	Untreated	107 ± 3.1	32.0 ± 0.8	32.0 ± 0.8	0.01 ± 0.05
	Plasma	57.4 ± 1.5	54.1 ± 1.1	40.5 ± 0.2	13.6 ± 0.8
	Plasma + precursor	33.0 ± 2.7	66.9 ± 1.7	38.8 ± 0.3	28.1 ± 1.4
	Plasma + primer	84.4 ± 4.9	40.7 ± 3.7	38.2 ± 2.3	2.42 ± 1.4
PCR30	Untreated	104 ± 0.6	32.7 ± 0.5	32.7 ± 0.5	0.01 ± 0.01
	Plasma	57.6 ± 1.3	53.9 ± 1.3	40.3 ± 0.5	13.6 ± 0.8
	Plasma + precursor	31.7 ± 3.4	68.6 ± 2.2	41.0 ± 0.5	27.6 ± 1.7
	Plasma + primer	84.5 ± 2.5	41.8 ± 1.3	39.7 ± 0.6	2.17 ± 0.7
PCR50	Untreated	104 ± 2.2	32.3 ± 0.3	32.2 ± 0.2	0.02 ± 0.05
	Plasma	55.9 ± 3.5	54.0 ± 3.3	39.0 ± 1.2	15.0 ± 2.1
	Plasma + precursor	50.3 ± 4.1	58.0 ± 3.4	40.4 ± 1.0	17.7 ± 2.4
	Plasma + primer	90.8 ± 3.2	39.8 ± 1.6	38.9 ± 1.1	0.89 ± 0.6

The untreated substrates have the largest contact angles (104-107°), and therefore the lowest γ_{tot} compared to the pretreated samples. All of the untreated samples have a very similar contact angle, but PIR30 has a somewhat higher one. Since the wettability decreases with increased contact angles, PIR30 shows slightly lower wettability among the untreated samples, worth noting is that the difference is very small. All the untreated samples have contact angles exceeding 90° which is the threshold for a surface to be considered hydrophobic. The reason behind the high contact angles and low γ_P for all untreated samples is that polypropylene is made of carbon and hydrogen atoms and therefore creates very hydrophobic surfaces. Dispersive forces dominate the interactions between carbon and hydrogen atoms, contributing almost entirely to the γ_{tot} .

When treating the materials with plasma, the contact angle decreases drastically to around 55-60°, where PCR50 has the lowest contact angle and virgin PP has the highest one among the materials. These surfaces then have a higher γ_{tot} than the untreated samples due to both a higher γ_P and γ_D . The γ_{tot} for these samples approaches the surface tension of water, and the surfaces can therefore interact with the water droplet to a higher extent, leading to a higher wettability. This also means that the adhesive will wet the surface better, which is favourable when bonding the polypropylene material. A decreasing contact angle, a higher γ_P , and a higher γ_{tot} are expected because of the properties of the plasma. Plasma treatment will alter the surface by adding polar functional groups to the surface. These polar groups will make the surface more hydrophilic, hence reducing the contact angle and resulting in a higher γ_P and γ_{tot} . This result shows that the plasma treatment works very similarly for all the materials, and that the difference between them is small. The same result has been seen in earlier studies, for example,

in one study by Encinas, Abenojar, and Martínez [39] discussed in chapter 3, where the γ_p drastically increased after plasma treatment, which in turn increased the total SFE (γ_{tot}) of their polypropylene surfaces.

The result from the pretreatment with plasma plus precursor shows similar trends as of the plasma-treated samples. However, the contact angle decreases even more after this pretreatment, to around 31-33° for PP, PIR30, and PCR30 but around 50° for PCR50. Worth noting is that these angles are below the recommended threshold for the polyurethane adhesive, according to technical regulations from Volvo. Same as for plasma, the γ_{tot} increases because of an increase of γ_p and γ_D . The epoxy end of the GLYMO molecule, facing the surface, is more polar and reactive than the polar groups of the plasma. This generates a higher γ_p for the plasma plus precursor compared to the plasma itself, which is also observed in Table 5.2. The contact angle is relatively low, and the polar contribution is high compared to the plasma-treated samples. Why PCR50 gains a higher contact angle and a lower γ_{tot} than the other materials can be due to several reasons. PCR50 contains a higher degree of recycled plastic than PIR30 and PCR30, which increases the possibility of a higher degree of contaminants, such as additives from earlier processes. Additionally, PCR is often regarded as a less pure plastic compared to PIR due to its post-consumer origin, which makes its quality harder to control. This can make it behave differently in contact with the GLYMO molecule. However, the standard deviation is highest for PCR50, so the high contact angle might as well be a coincidence.

The plasma plus primer pretreatment resulted in contact angles between 84-94° for all materials, meaning they meet or exceed the hydrophobicity threshold of surfaces. In total, the contact angles for the primer decreased to a lesser extent than those with plasma treatment. The primer is a polymeric material based on polyisocyanate and is applied on top of the plasma, covering the polar groups generated by the plasma treatment. However, the polyisocyanate-based primer does have polar isocyanate groups, which will contribute to the γ_p . γ_p for the plasma plus primer samples is, in fact, lower than the ones for the plasma-treated surfaces. This means that the plasma treatment generates more polar functional groups than the primer does, which may enhance the adhesion and generate a higher strength of the bonded polypropylene. However, the primer thus generates a higher γ_p than for the untreated samples, which is expected due to the polar isocyanate groups of the primer. This means that the γ_{tot} for the primed surfaces is higher than that of the untreated samples but lower than the plasma-treated samples.

5.3 Surface roughness

The results from the surface roughness measurements are presented in Figure 5.1 down below. PP received the highest value of both R_a and R_z , which shows that PP has the roughest surface. PIR30 has the lowest values for both R_a and R_z , which indicates that PIR30 has the smoothest surface. Since PP and PCR30 have slightly higher values compared to the others, there may be an increase in adhesion strength for these materials because the surface area increases with higher surface roughness. However, the differences between the materials' values are low, indicating that their surface roughness is relatively similar. The difference in R_a and R_z values between the materials may be due to local irregularities, and these small differences may not affect the adhesion.

The standard deviations observed for PP, PCR30, and PCR50 are relatively high. Although increasing the number of replicates could statistically reduce the standard deviation, the presence of local surface irregularities remains a significant factor. Due to the inherently low R_a and R_z values of these materials, even small topographical deviations can disproportionately affect the results, leading to significantly higher individual readings and a larger standard deviation.

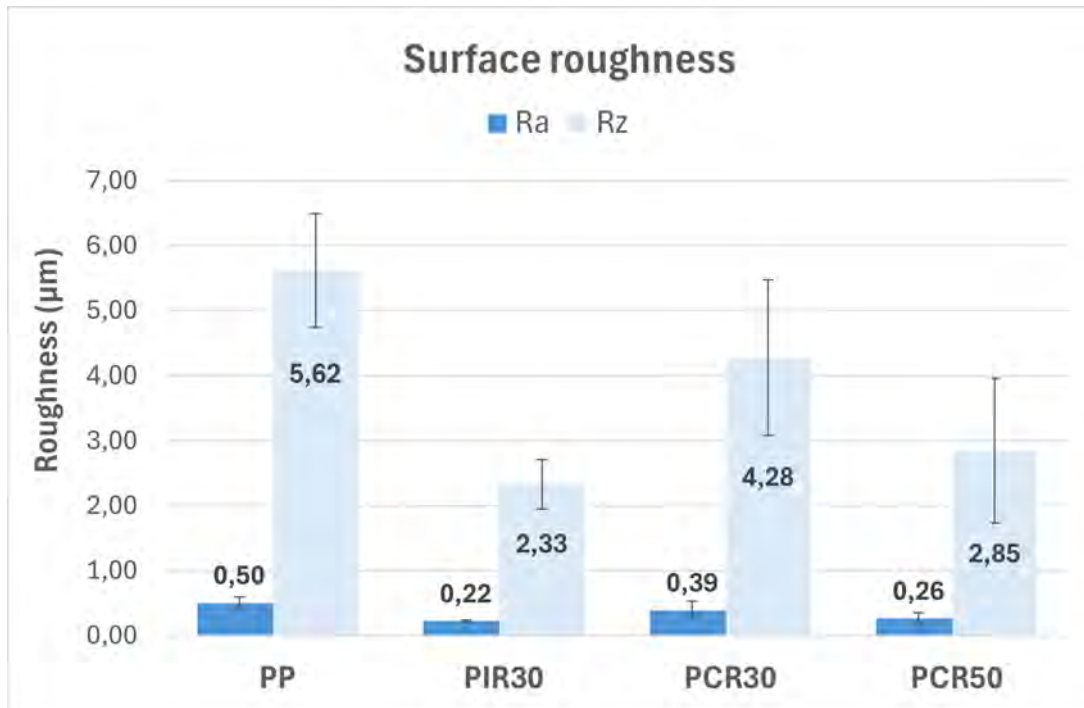


Figure 5.1: The average values of the parameters R_a and R_z for each material without pretreatment. The average and the standard error are based on five measurements on each plastic. R_a is the roughness average and R_z is the mean roughness depth.

5.4 Failure of samples

From the start, the idea was to apply the primer directly on the coupons after wiping the surface with isopropanol. However, it was discovered that the primer did not adhere properly to the substrate, and the coupons failed during assembly because of little or no adhesion between the primer and the plastic surface. The method was then updated, and plasma treatment was performed before the primer was applied. The untreated samples had the same results, with no proper adhesion and failed during assembly. Thus, the two initials of PCR50 did not completely fail, and the strength of them could be measured, but the values ended up very low, and these two results were therefore neglected in the diagrams. Therefore, no tropical or heat ageing was performed for the untreated samples, nor any LSS tests. Additionally, three of the plasma plus precursor samples failed during assembly and did not undergo any LSS tests.

5.5 Lap shear strength testing

In the following section, all the LSS results for each material and pretreatment are presented.

5.5.1 PP

The result from the lap shear testing of the PP coupons is seen in Figure 5.2. The plasma-treated PP has overall the highest strength, and the plasma plus precursor has the lowest strength. The high strength of the samples with plasma is expected due to the introduction of reactive polar groups from the plasma, which promotes high adhesion between the plastic surface and the polyurethane adhesive.

The low strength of the plasma plus precursor, however, is not expected because the combination of plasma and a customised precursor should theoretically promote better bonding. This is probably due to a methodological mismatch, as all samples with this pretreatment, regardless of material, show low strength. Either the plasma parameters are not optimised for the experiment, or the GLYMO molecule is not compatible with the combination of the polyurethane adhesive and polypropylene. The thickness of the GLYMO molecule layer is also relevant to discuss. The applied layer is likely too thick, which may increase the risk of internal shear force developing within the precursor bulk. This can be adjusted by increasing the distance between the jet head and the substrate, reducing the precursor flow, or raising the application speed. Another aspect to consider is that the contact angle decreases drastically after the plasma plus precursor pretreatment, and the polar contribution becomes very high, see section 5.2. These values are below the thresholds for contact angles and surface free energy by Volvo Cars' technical regulations, and therefore may affect the adhesion.

All the plasma-treated samples and the plasma plus primer T display structural bonding. For both plasma and plasma plus primer treatments, the strength increases progressively from the initial state to heat ageing, and further to tropical ageing. This can be explained by the post-curing effect, which means that the adhesive cures even more after the first curing cycle. This phenomenon is due to the rising temperature for heat ageing and the combination of elevated temperature and high humidity for tropical ageing. Probably, the temperature rise accelerates the chemical reaction to some extent in both cases. The moisture from the tropical ageing penetrates the joint and the free isocyanates, which have not yet reacted with polyol molecules, instead react with water molecules [45]. The isocyanate and water molecules react and form carbamic acid, which decomposes into amines and carbon dioxide, and lastly end up in urea formation. In this way, these urea bonds will contribute to the hardening of the adhesive further. The chemical primer is also based on isocyanates and may further enhance the post-curing effect when the isocyanates react with the water molecules. A more detailed study of the molecules and bonds in question can be done using FTIR analysis.

For the plasma plus precursor-treated samples, the strength trend is reversed, with the initial series exhibiting the highest strength and the tropical-aged ones the lowest. However, the overall strength values and the differences between them are considerably small, making it difficult to draw definitive conclusions about the effects of post-curing on these coupons. Heat and humidity may interfere with the GLYMO molecule, potentially affecting its bonding to the plastic substrates.

The standard deviations are generally similar for all the samples, except for plasma H and plasma plus precursor H, in comparison to the sizes of their bars. A high standard deviation for the heated plasma is due to one sample with high strength, and the standard deviation for plasma plus precursor is high because of one very low sample compared to the others. They both contain one outlier each, and the standard deviation would be significantly lower if the outliers were removed. More replies of each series would probably also affect the standard deviation for all the materials.

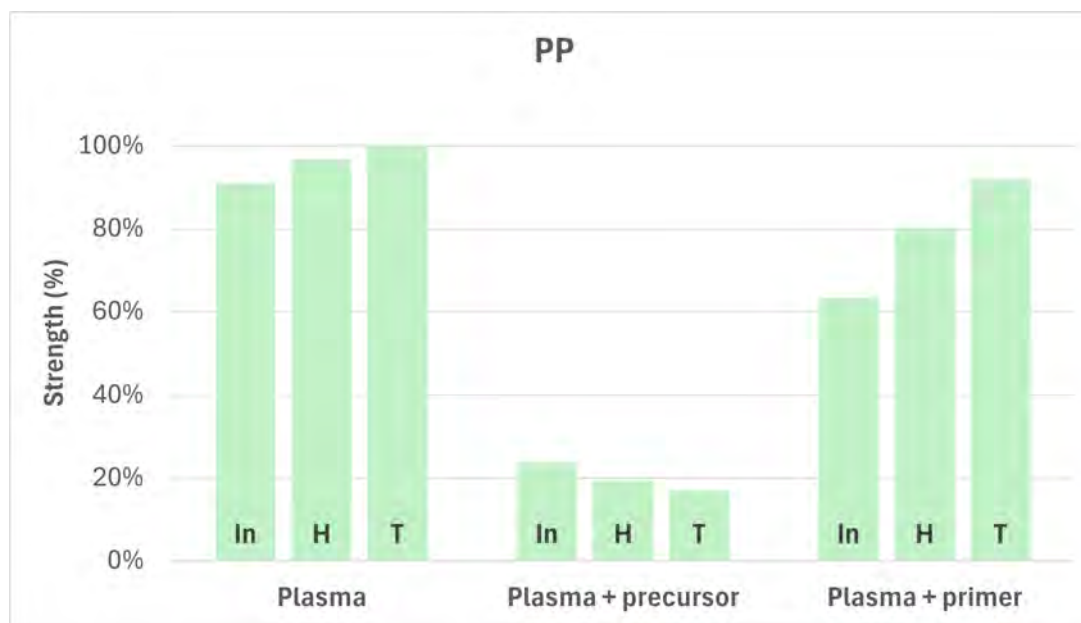


Figure 5.2: The averages of lap shear strength (in %) for all pretreatments of PP. The percentages are calculated based on the highest series average strength within the PP material. The average within each series is calculated based on five samples. The abbreviation *In* stands for initial (no ageing), *H* for heat ageing, and *T* for tropical ageing.

The failure modes of the PP coupons are presented in Figure 5.3, and pictures of the coupons are seen in Figure A.1 in Appendix A. All the initial and tropical-aged plasma-treated sample results in SF. The heat-aged plasma-treated samples result in SF, AF, and the combination SF/AF. This difference in failure mode after heat ageing can be due to secondary crystallisation of the polymer [49]. This makes the material stiffer and increases the material's strength due to a higher degree of crystallinity. More crystalline surfaces may, however, cause problems during bonding to the adhesive because the polymer chains have less mobility and a lower possibility to entangle and chemically interact with the adhesive. As a result, the adhesive is more likely to become the weak point, causing the heat-aged samples to exhibit AF instead of SF, as the initial ones. Another reason behind the result of the heat-aged series may be exudation of additives, for instance, release agents migrating to the surface, causing lower adhesion between the adhesive and the substrate. Exudation and secondary crystallisation may occur simultaneously, causing a change in failure modes and making it difficult to determine each contribution.

All the coupons pretreated with plasma plus precursor yield AF regardless of ageing. The initial and heat-aged coupons from plasma plus primer receive DF. The tropical-aged samples, on the other hand, result in SF, which may also be explained by post-curing of the adhesive in the

humid climate, which makes the substrate the weakest point. The changes in failure modes after the ageing procedures within the same pretreatment can be explained by the influence of different parameters, all affecting the samples at the same time. It is difficult to draw any conclusions about what actually happens without performing any further analysis, for example, using differential scanning calorimetry (DSC).

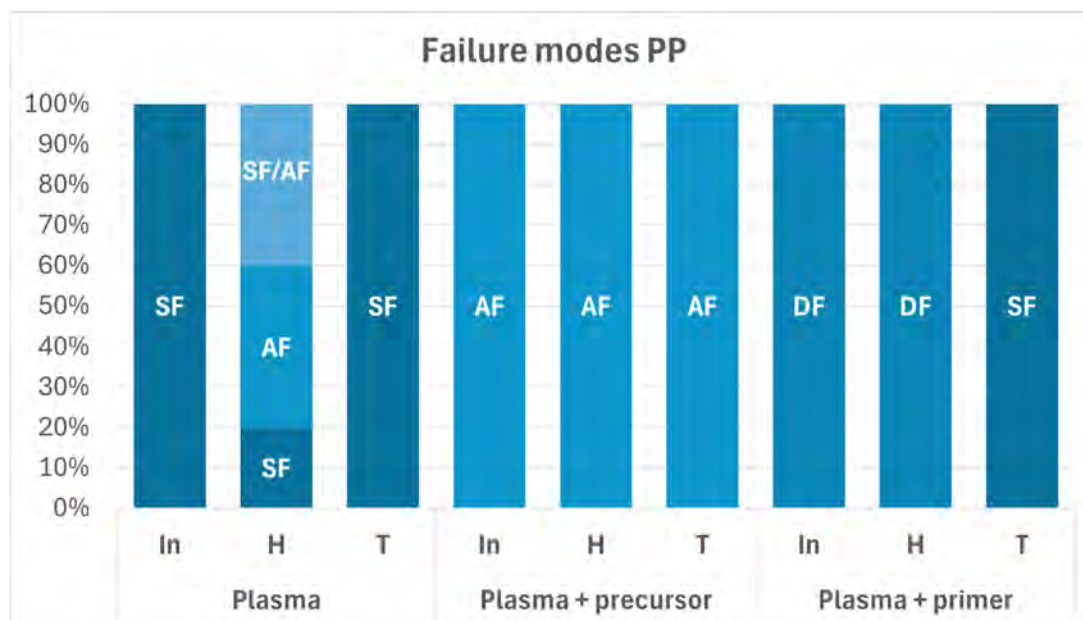


Figure 5.3: Failure modes for all PP samples. SF is substrate failure, AF is adhesion failure, and DF is delamination failure. SF/AF is a combination of SF and AF happening at the same time.

5.5.2 PIR30

All the plasma-treated PIR30 coupons receive high strength and structural bonding, see Figure 5.4. The ageing procedures do not contribute to a higher strength as it does for PP, with a small or no influence from the post-curing effect received during tropical and heat ageing. The result displays a slightly lower strength after heat ageing, which may be due to exudation of additives, but the differences among them are small.

All three series with plasma plus precursor as pretreatment show low strengths. Here, the strengths become progressively lower for the heat and tropical aged coupons compared to the initial ones, so there was no visible post-curing effect. The reason behind this is not clear, but one suggestion is that the function of the GLYMO molecule is suppressed during ageing. For the plasma plus primer-treated coupons, only the tropical ageing shows the strength of structural bonding. The strength increases markable for both the heat and tropical aged series due to post-curing. Plasma plus primer In shows a higher standard deviation compared to the rest of the series within PIR30, although the difference is not particularly large.

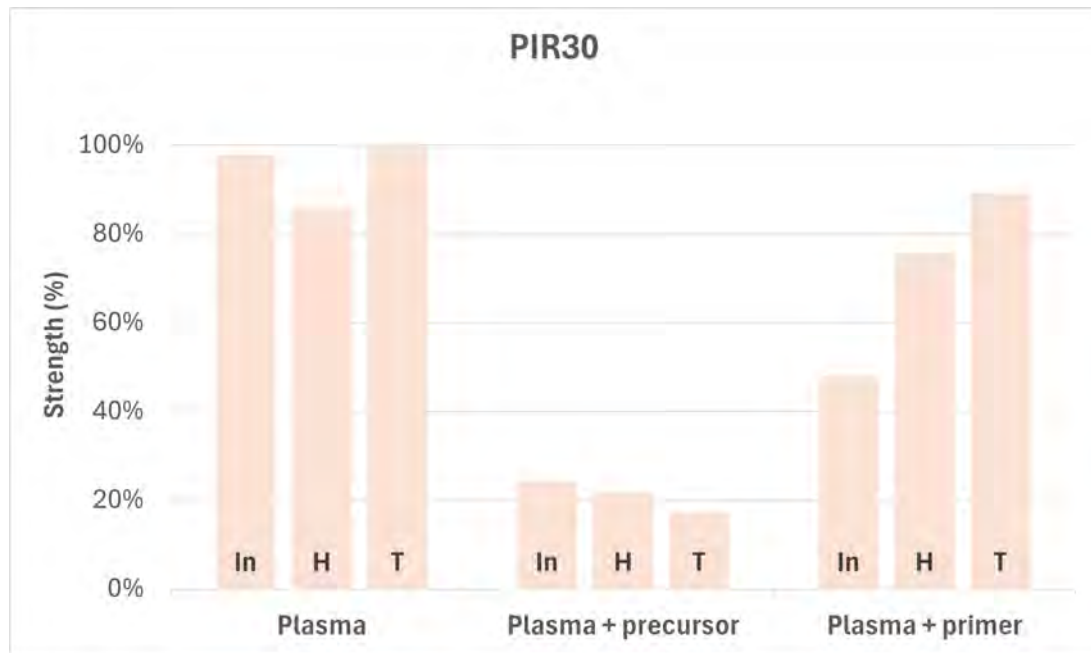


Figure 5.4: The averages of lap shear strength (in %) for all pretreatments of PIR30. The percentages are calculated based on the highest series average strength within the PIR30 material. The average within each series is calculated based on five samples, except for plasma + precursor In and H, where the average is based on four samples. The abbreviation *In* stands for initial (no ageing), *H* for heat ageing, and *T* for tropical ageing.

All the plasma-treated coupons result in the failure mode SF, and all the plasma plus precursor coupons receive AF, see Figure 5.5. Here, the exudation, secondary crystallisation, or post-curing did not affect the failure mode after ageing. Rather, the substrate of the plasma H sample has decreased in strength, and the material itself has changed during the heat ageing. However, the failure mode is different among the initial and the aged samples of plasma plus primer, where the initial displays DF, the heat aged yield DF and SF, and the tropical aged exhibit SF. The occurrence of SF for plasma plus primer T may be due to stronger adhesion resulting from the post-curing effect, causing the substrate to become the weak point. Pictures of all PIR30 coupons can be seen in Figure A.2 in Appendix A.

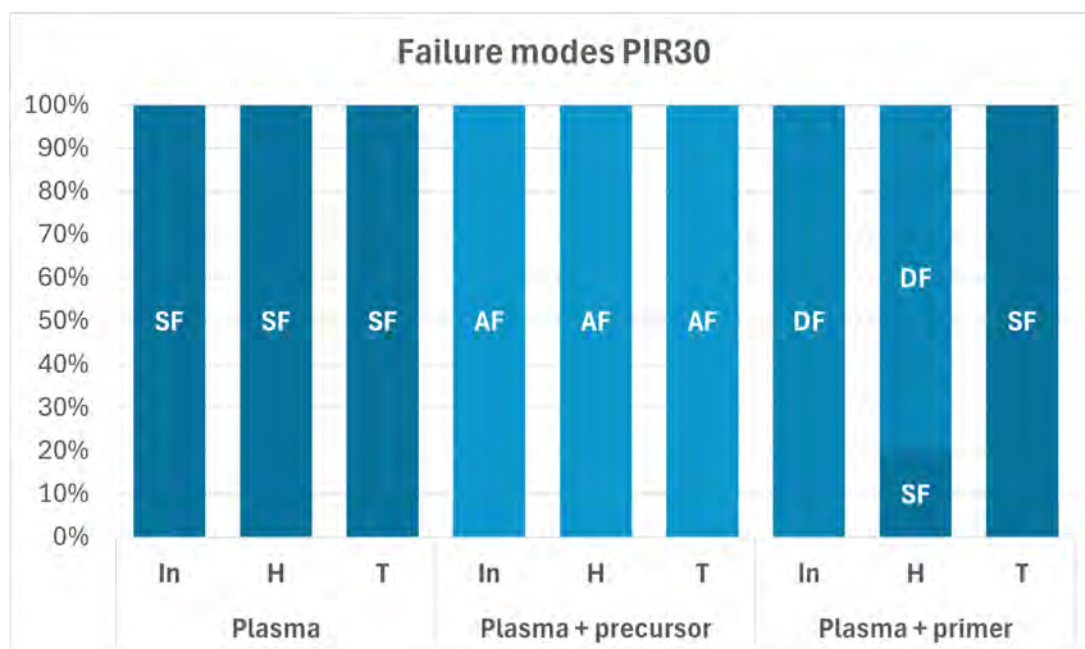


Figure 5.5: Failure modes for all PIR30 samples. SF is substrate failure, AF is adhesion failure, and DF is delamination failure. Note that plasma + precursor In and H are based on four samples in each series instead of five.

5.5.3 PCR30

As for the other materials, the plasma-treated coupons receive relatively high strength, showing structural bonding, see Figure 5.6. In this case, the initial series exhibits the highest strength, while the tropical and heat-aged samples show slightly lower strengths. Therefore, the post-curing effect is less pronounced, and it may have caused some exudation of additives for both series, resulting in a decrease in strength. The coupons treated with plasma plus precursor remain in low strength and show no structural bonding. The heat-aged have slightly higher strength than the others, and the tropical have the lowest, but they are very similar, and no statements about the post-curing effect can be made. Plasma plus primer T holds a high strength compared to the initial and heat-aged series for the same pretreatment. Similar to the plasma-treated samples, this series also exhibits structural bonding. The increase in strength after tropical ageing clearly indicates that the post-curing effect has a significant impact in this case. Overall, the standard deviations differ with small variations, from very small to visible deviations. The standard deviation for plasma plus precursor In is notable compared to the size of the bar. However, there are no distinct major deviations that need to be taken into account.

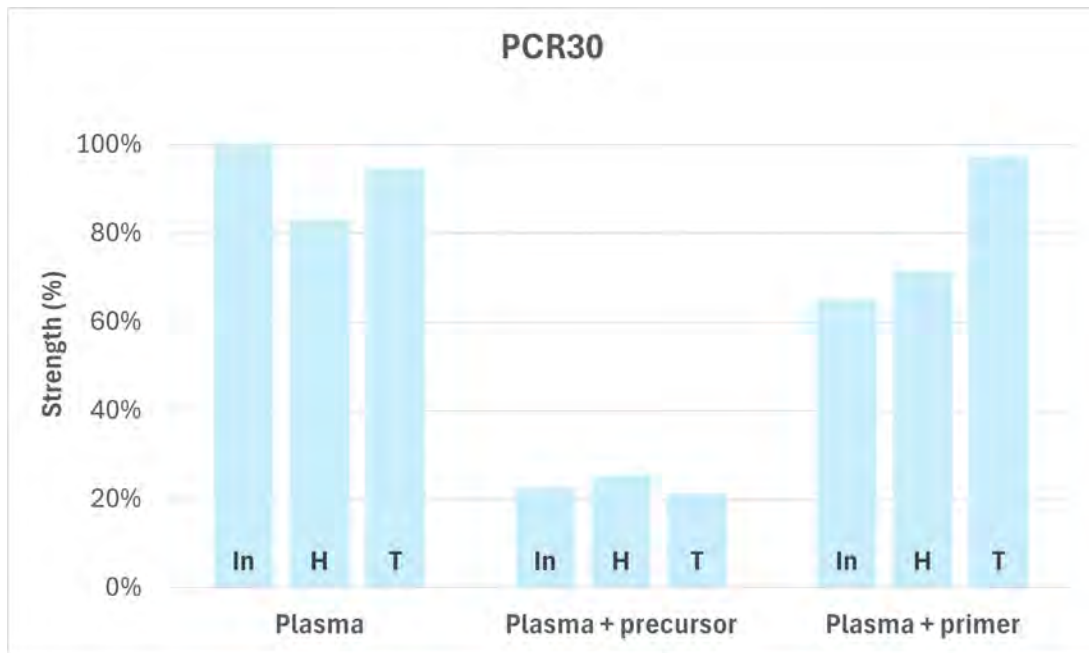


Figure 5.6: The averages of lap shear strength (in %) for all pretreatments of PCR30. The percentages are calculated based on the highest series average strength within the PCR30 material. The average within each series is calculated based on five samples, except for plasma + precursor T, where the average is based on four samples. The abbreviation *In* stands for initial (no ageing), *H* for heat ageing, and *T* for tropical ageing.

The failure mode for the plasma-treated coupons changes to some extent upon heat ageing but remains with SF after tropical ageing, see Figure 5.7. As discussed earlier, the change from SF to AF or a combination of AF/SF is probably due to exudation of additives or secondary crystallisation happening during heating. However, the absence of increased strength after heat ageing reduces the likelihood of secondary crystallization and may indicate that exudation is the most prominent. The failure mode is AF for all the plasma plus precursor-treated coupons as previously. This further demonstrates the weak adhesion of these samples. The initials of the plasma plus primer coupons and the majority of the heat-aged results in DF. In contrast, the tropical aged samples give rise to SF. This result is probably due to post-curing of the adhesive in the humid climate, which instead makes the substrate the weakest point, which is also demonstrated by the high strength. Pictures of all PCR30 coupons can be seen in Figure A.3 in Appendix A.

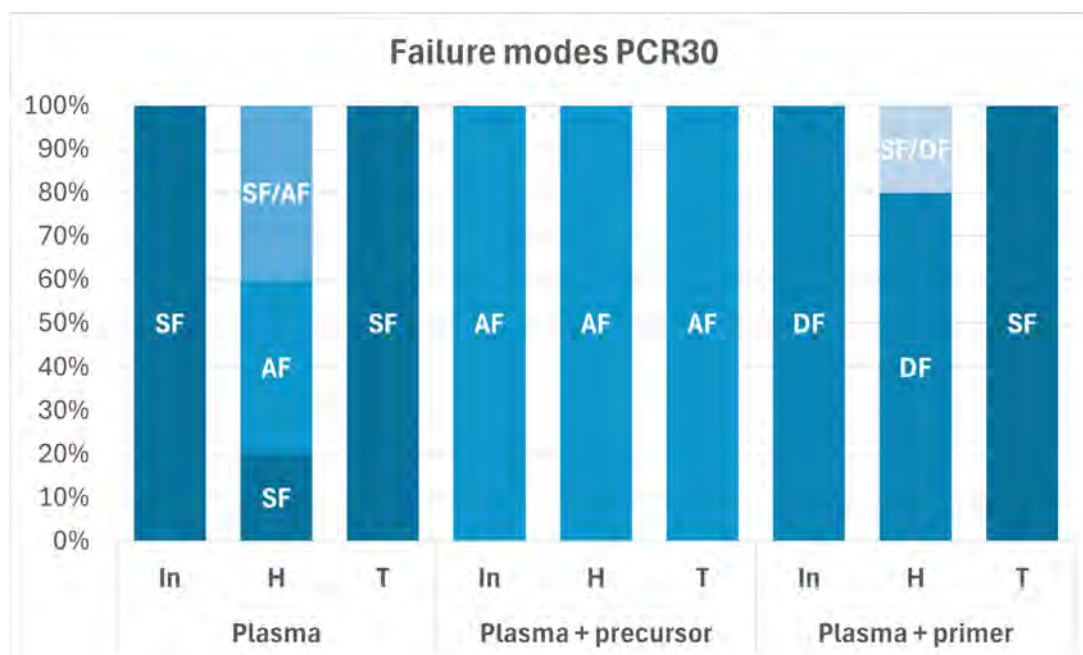


Figure 5.7: Failure modes for all PCR30 samples. SF is substrate failure, AF is adhesion failure, and DF is delamination failure. SF/AF and SF/DF combinations of failure modes that happen at the same time. Note that plasma + precursor T is based on four samples in the series instead of five.

5.5.4 PCR50

Both the plasma In and plasma T series show strengths of structural bonding, see Figure 5.8. The increased strength of plasma T may once again be due to post-curing of the adhesive. The plasma H series has strength below structural bonding, and this lower strength can be explained by exudation of additives in the heated climate. As in previous cases, the plasma plus precursor receives the lowest strength of them all, with small differences between the initial and aged samples. The tropical-aged series has the lowest strength among them all, and therefore, no distinct post-curing is seen. The initials and heat-aged plasma plus primer-treated coupons show similar strength below the threshold for structural bonding, and no exudation of additives is prominent. The tropical-aged series receives the highest strength of all treatments of PCR30 and indicates structural bonding. The high strength is motivated by extensive post-curing in the humid climate. The standard deviations are relatively small with minor variations.

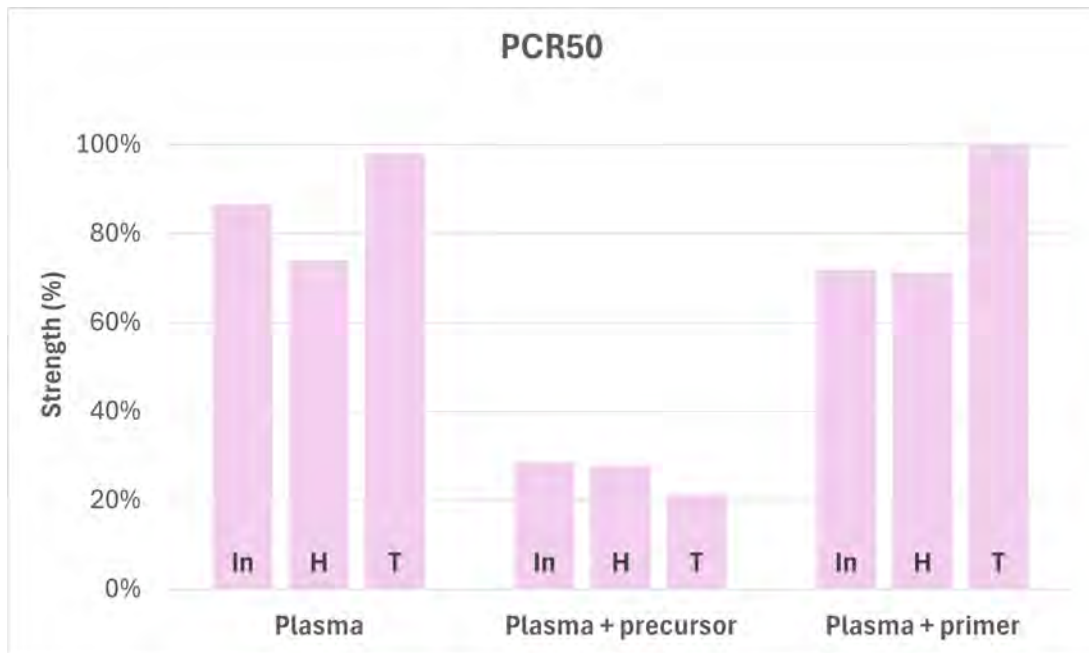


Figure 5.8: The averages of lap shear strength (in %) for all pretreatments of PCR50. The percentages are calculated based on the highest series average strength within the PCR50 material. The average within each series is calculated based on five samples. The abbreviation *In* stands for initial (no ageing), *H* for heat ageing, and *T* for tropical ageing.

The failure modes for PCR50 are seen in Figure 5.9, and pictures of the coupons can be found in Figure A.4 in Appendix A. All the initial and the majority of the heat-aged plasma-treated samples receive AF, except for one heat-aged sample exhibiting SF. The tropical-aged series results in SF, likely due to post-curing of the adhesive and the substrate becoming the weak point. The plasma plus precursor-treated samples all exhibit the failure mode AF, which aligns with the other materials within the same pretreatment described in the sections above. The series of plasma plus primer *In* and the majority of plasma plus primer *H* generates DF. The tropical-aged samples results in SF, which may be explained by post-curing of the adhesive and hence a higher adhesion strength.

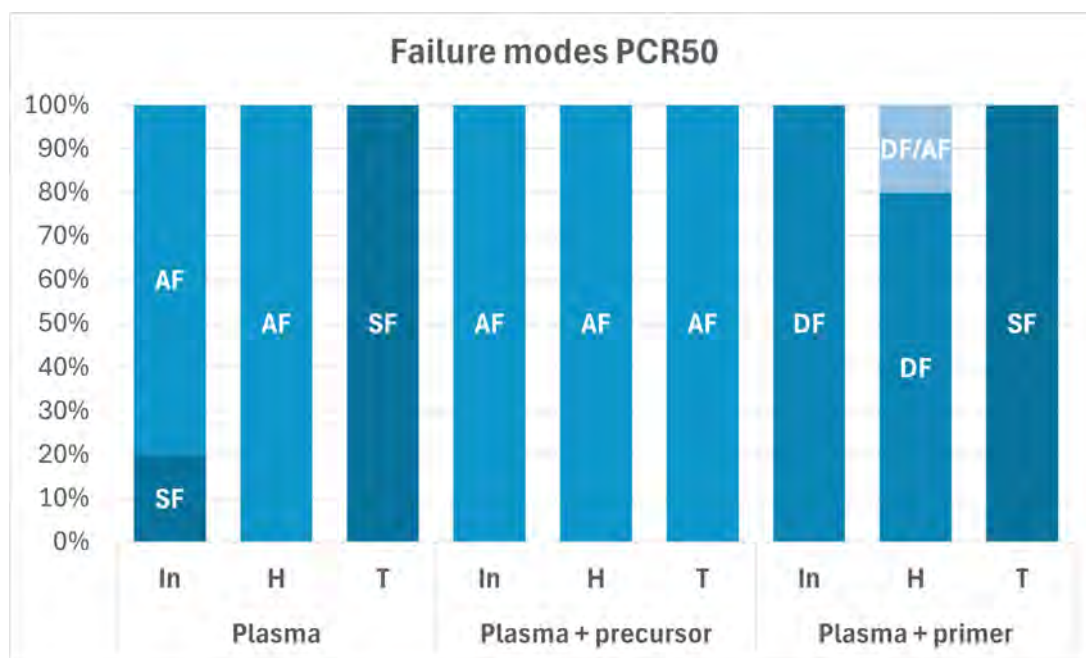


Figure 5.9: Failure modes for all PCR50 samples. SF is substrate failure, AF is adhesion failure, and DF is delamination failure. DF/AF is a combination of DF and AF that is happening at the same time.

5.5.5 Comparison of the materials with plasma treatment

The plasma-treated samples have the highest strength overall, and plasma was the only pretreatment where all series, except the heat-aged PCR50, aligned with Volvo Cars' requirements. This pretreatment is the most preferable to use in Volvo's production because of its simplicity, cleanliness, and environmental advantages. Therefore, it is of high interest to compare the plastics treated with plasma, see Figure 5.10 for LSS results and Figure 5.11.

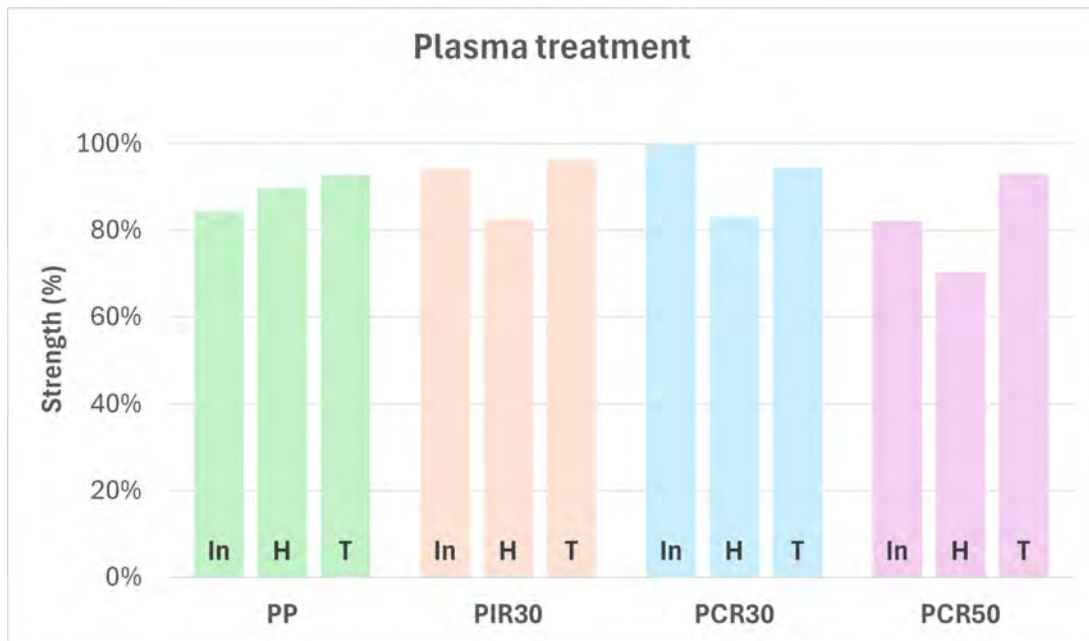


Figure 5.10: The averages of lap shear strength (in %) for the plasma-pretreatments of PP, PIR30, PCR30, and PCR50. The percentages are calculated based on the highest average strength of all plasma series. The average within each series is calculated from five samples. The abbreviation *In* stands for initial (no ageing), *H* for heat ageing, and *T* for tropical ageing.

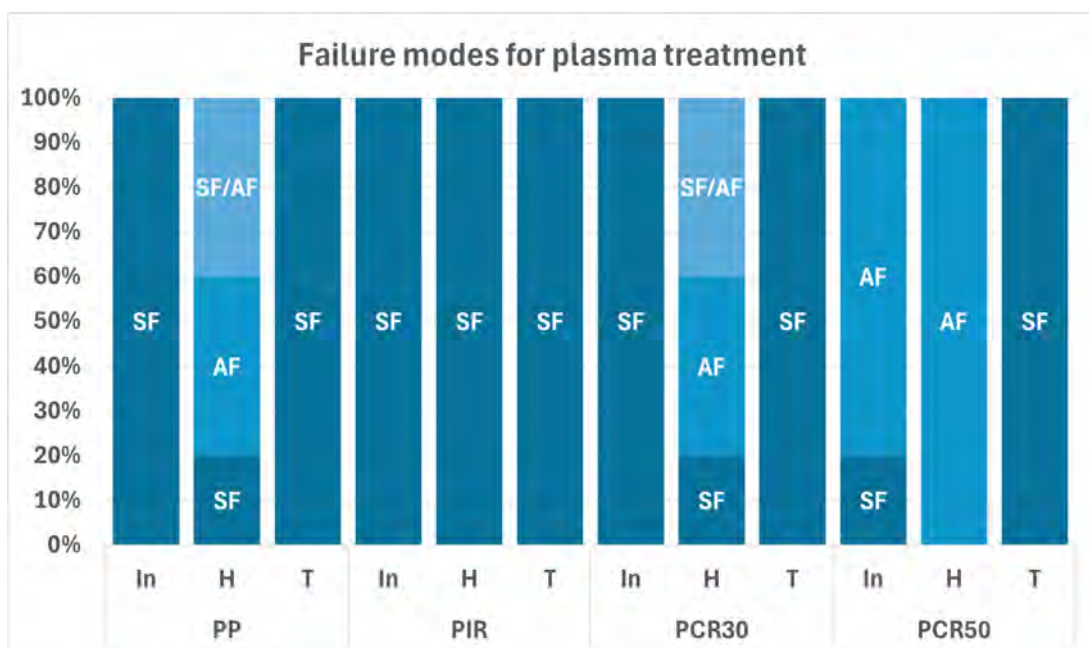


Figure 5.11: The failure modes of all the plasma-treated samples. SF is substrate failure, AF is adhesion failure, and DF is delamination failure. SF/AF is a combination of SF and AF happening at the same time.

All test, except for PCR50 H, shows strengths indicating structural bonding [43]. The three recycled materials show similar trends among the different ageing procedures, where the heated samples have the lowest strengths among them all. The difference in this trend between recycled and virgin plastics could be due to the higher concentration of additives in recycled materials, which are more likely to exude. For PP, the initial sample has the lowest strength, and the heated sample is between the initial and tropical. Generally, all the coupons after tropical ageing receive very high strength. This can be explained by the post-curing effect of the adhesive occurring during high humidity and elevated temperature. During post-curing, the curing and hardening of the adhesive will be accelerated by the favourable climate, see subsection 5.5.1 for a deeper explanation.

PIR30 and PCR30 perform with similar strengths and, in some cases, even better than PP with structural bonds. This makes PIR30 and PCR30 very promising as substitutes for virgin PP in the electrical vehicle battery package. In the case of PCR50, when the recycled content reaches 50 %, it shows slightly lower strengths and therefore requires more development of the method to include this high percentage of recycled material in the production.

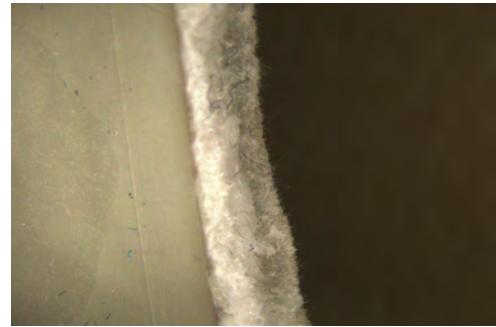
5.6 Study of cross-section of the coupons

The cross-sections of the different materials, studied in the microscope, are seen in Figure 5.12. The pictures on the left were captured from above to highlight differences in the bulk material, while the pictures on the right were taken from the side to provide a clearer view of the surface structure.

The surfaces in the cross-sections appear irregular and fibrous, with visible glass fibres protruding from the matrix, see Figure 5.12b, Figure 5.12d, Figure 5.12e, and Figure 5.12h. The glass fibres are relatively evenly distributed through the matrix with some changes in the centre, which explains the whiteness visually in the coupons, see Figure 5.12a, Figure 5.12c, Figure 5.12e, and Figure 5.12g. The orientation of the fibres seems to be random, however, a deeper scan is preferable to investigate a more accurate orientation of the individual fibres. There is no significant difference among the materials noticed. Additionally, no visible glass fibres protrude from any of the bonding surfaces, which is unlikely to affect the adhesion.



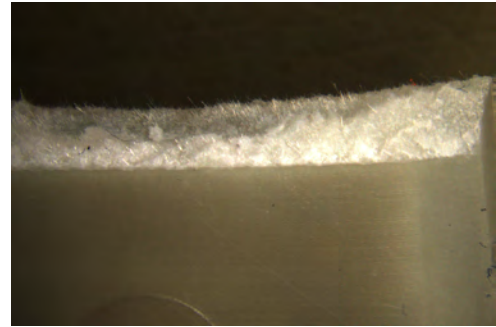
(a) PP



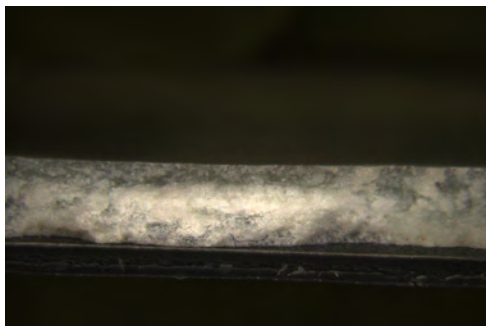
(b) PP



(c) PIR30



(d) PIR30



(e) PCR30



(f) PCR30



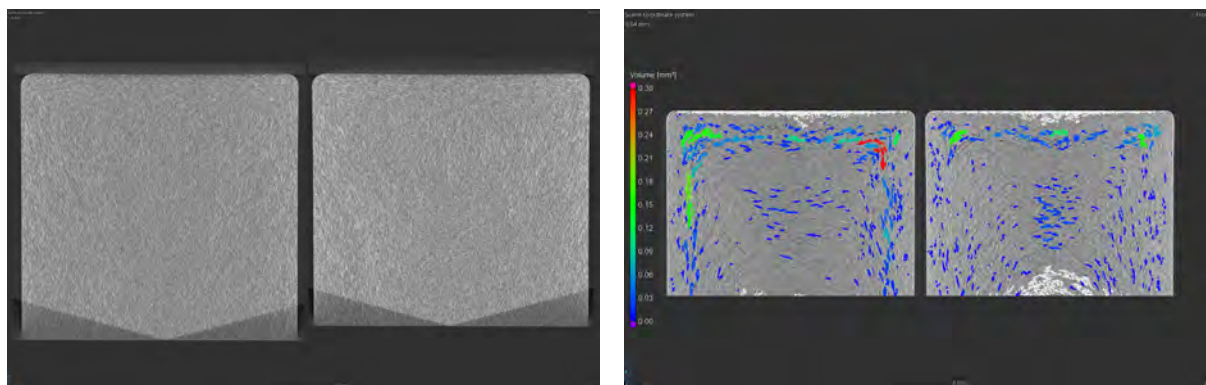
(g) PCR50



(h) PCR50

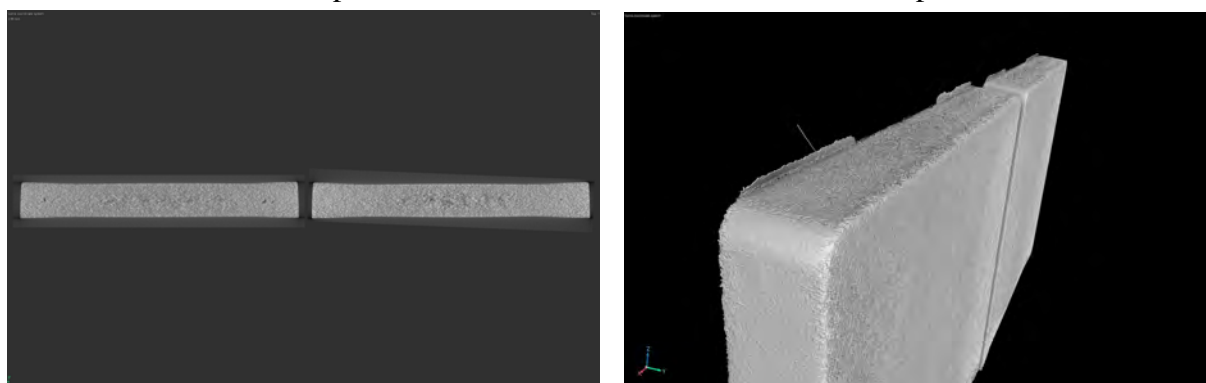
Figure 5.12: Microscopic pictures of the cross sections. The pictures on the left were captured from above and the pictures on the right were taken from the side to provide different views of the surface structure.

The complementary results from the CT scan of PP and PIR30 show that the glass fibres are evenly distributed at the surface, see Figure 5.13a and Figure 5.13d. Voids or irregular density within the bulk material are visible in the centre and close to the edges of both matrices, see Figure 5.13b with coloured voids and Figure 5.13c. The glass fibres can freely orient in different directions in these areas, which creates the whiteness seen in the middle of all the coupons. Anyhow, these irregularities are not seen on the surface and will not affect the adhesion.



(a) The surface of the coupons.

(b) The bulk of the coupons.



(c) The cross-section of the coupons.

(d) The surface topography.

Figure 5.13: The result from the CT scan of PP to the left and PIR30 to the right in each figure.

6

Conclusion

When studying the adhesion of recycled polypropylene and their possibility to substitute virgin PP, the mechanical and physical properties of the bonds were key factors in the comparison to the virgin PP. In conclusion, the recycled materials PIR30 and PCR30 showed similar high adhesion and strong structural bonding as PP after plasma pretreatment and are therefore possible substitutes for virgin PP in the application of electrical vehicle battery packages based on the results in the project. The material PCR50 shows promising results, showing slightly lower strength than virgin PP, PIR30, and PCR30. The 50 % proportion of recycled material, for PCR50, has a significant impact on the bond line performance, which makes it more complicated to handle during production. Anyhow, PCR50 still shows very promising results and may be used as an alternative for virgin PP in the future after some adjustments. A suggestion is to implement a lower proportion of recycled plastic, like 10-30 %, and gradually increase the recycled content.

It is proven that pretreatment of the plastic surfaces is necessary regardless plastic, and plasma-treatment is considered the most effective pretreatment of the ones investigated in this project. The majority of the coupons with other pretreatments investigated, including plasma plus primer and plasma plus precursor, did not result in strong structural bonds and require further optimisation before being considered viable. However, plasma-pretreatment exclusively is superior because of its simplicity, cleanliness, and environmental benefits for both nature and workers.

Furthermore, it is of high importance to study more replicates of the coupons to ensure that the bond line strength of the recycled materials is both consistent and sufficient before implementation into production.

7

Future Outlooks

One interesting future outlook is to investigate what the PIR and PCR plastic contain, including the type of additives and fillers, for example and their proportion. Additionally, an extensive study of the distribution and orientation of the glass fibres is also of interest. This knowledge may give a better understanding of the materials' chemical and mechanical properties. Another interesting aspect to further improve the method is to optimise the plasma parameters for the recycled materials. Examples of adjustments that can be made are changing the distance to the substrate, the speed, or the plasma jet head.

In this study, it was noticed that ageing may have an impact on the additive exudation to the surfaces of the coupons and the crystallinity of the bulk material. Therefore, it would be interesting to study the surfaces of the plastics in depth and how the surface properties are affected by heat and tropical ageing. One way of doing so is to perform FTIR analysis on the surfaces after ageing and analyse if and which substances migrate to the surface. Additionally, DSC can complement the FTIR analysis to see the differences in melting behaviours and crystallinity. How the polymer chain orientation is affected by the ageing is also of interest and may affect the materials' mechanical properties.

An important step in product development is to have methods for quality assurance. In order to manufacture and produce cars with recycled plastic in the battery package, the company must have regulations to guarantee the quality and properties of the materials. Key questions that must be addressed are; what requirements should be established and how could these requirements be verified and monitored. Volvo Cars has specifications regarding recycled materials that address general statements and requirements. Every batch of the recycled plastic must be controlled to fulfil these statements and requirements. However, recycled plastics have not been utilised in the battery package before, so it is important to examine these existing regulations and adjust them to the future battery package.

Bibliography

- [1] *Battery cell-to-body for future Volvo cars on SPA3 architecture - animation*, en-gb. [Online]. Available: <https://www.media.volvocars.com/global/en-gb/media/videos/333599/battery-cell-to-body-for-future-volvo-cars-on-spa3-architecture-animation> (visited on 05/07/2025).
- [2] Copernicus Climate Change Service, *Global climate highlights 2024*, Jan. 2025. [Online]. Available: <https://climate.copernicus.eu/global-climate-highlights-2024> (visited on 02/06/2025).
- [3] *Plastics*, en, European Environment Agency, Nov. 2024. [Online]. Available: <https://www.eea.europa.eu/en/topics/in-depth/plastics> (visited on 01/24/2025).
- [4] *Volvo Cars siktar på att kunna använda minst 25 procent återvunnen plast i varje ny bil från 2025*, sv, Volvo Car Sverige AB. [Online]. Available: <https://www.media.volvocars.com/se/sv-se/media/pressreleases/230703/volvo-cars-siktar-pa-att-kunna-anvanda-minst-25-procent-atervunnen-plast-i-varje-ny-bil-fran-2025> (visited on 01/24/2025).
- [5] *Sustainability is as important to us as safety | Volvo Cars*, en. [Online]. Available: <https://www.volvocars.com/intl/sustainability/circular-economy/> (visited on 01/24/2025).
- [6] L. A. Castonguay and A. K. Rappe, "Ziegler-Natta catalysis. A theoretical study of the isotactic polymerization of propylene," en, *Journal of the American Chemical Society*, vol. 114, no. 14, pp. 5832–5842, Jul. 1992. DOI: 10.1021/ja00040a053.
- [7] A. Schon, "Stereospecificity," *Science*, vol. 148, no. 3668, pp. 401–411, 1965. DOI: 10.1126/science.148.3668.401.
- [8] J. Karger-Kocsis, "Tacticity, Regio and Stereoregularity," eng, in *Polypropylene Handbook: Morphology, Blends and Composites*. Cham: Springer, 2019, ch. 1, pp. 1–29.
- [9] T. Parenteau, G. Ausias, Y. Grohens, and P. Pilvin, "Structure, mechanical properties and modelling of polypropylene for different degrees of crystallinity," *Polymer*, vol. 53, no. 25, pp. 5873–5884, 2012. DOI: <https://doi.org/10.1016/j.polymer.2012.09.053>.
- [10] J. Cowie and V. Arrighi, "Polymerization Reactions Initiated by Metal Catalysts and Transfer Reactions," en, in *Polymers: Chemistry and Physics of Modern Materials*, 3rd ed. CRC Press, Jul. 2007, ch. 7, pp. 175–196.
- [11] H. A. Maddah, "Polypropylene as a promising plastic: A review," *American Journal of Polymer Science*, vol. 6, pp. 1–11, 1 2016. DOI: 10.5923/j.ajps.20160601.01.

- [12] J. Cowie and V. Arrighi, "Polymer Stereochemistry," en, in *Polymers: Chemistry and Physics of Modern Materials*, 3rd ed. CRC Press, Jul. 2007, ch. 6, pp. 157–175.
- [13] M. Biron, "1 - outline of the actual situation of plastics compared to conventional materials," in *Thermoplastics and Thermoplastic Composites (Second Edition)*, ser. Plastics Design Library, M. Biron, Ed., Second Edition, William Andrew Publishing, 2013, ch. 1, pp. 1–29. [Online]. Available: <https://www.sciencedirect.com/science/article/pii/B9781455778980000019> (visited on 02/14/2025).
- [14] "Fiber-Reinforced Composites," in *Functional polymers*, ser. Polymers and Polymeric Composites: A Reference Series, M. A. J. Mazumder, H. Sheardown, and A. Al-Ahmed, Eds., Cham: Springer, 2019, ch. 11, pp. 417–446.
- [15] *The cell contacting system as an important component in the battery module - AKE technologies GmbH ENG*. [Online]. Available: <https://www.ake-technologies.com/news/146-the-cell-contacting-system-as-an-important-component-in-the-battery-module> (visited on 02/20/2025).
- [16] S. Arora, W. Shen, and A. Kapoor, "Review of mechanical design and strategic placement technique of a robust battery pack for electric vehicles," *Renewable and Sustainable Energy Reviews*, vol. 60, pp. 1319–1331, 2016. DOI: <https://doi.org/10.1016/j.rser.2016.03.013>.
- [17] "The Complete Injection Molding Process," in *Injection Molding Handbook*, D. V. Rosato, D. V. Rosato, and M. G. Rosato, Eds., 3rd ed., Boston, MA: Springer US, 2000, ch. 1, p. 4. [Online]. Available: <http://link.springer.com/10.1007/978-1-4615-4597-2> (visited on 02/20/2025).
- [18] T. Li, "Powder injection molding of metallic parts and structures," in *Encyclopedia of Materials: Metals and Alloys*, F. G. Caballero, Ed., Oxford: Elsevier, 2022, pp. 401–416. DOI: <https://doi.org/10.1016/B978-0-12-819726-4.00015-6>. [Online]. Available: <https://www.sciencedirect.com/science/article/pii/B9780128197264000156>.
- [19] V. Marturano, P. Cerruti, and V. Ambrogi, "Polymer additives," *Physical Sciences Reviews*, vol. 2, no. 6, Jun. 2017. DOI: [10.1515/psr-2016-0130](https://doi.org/10.1515/psr-2016-0130).
- [20] J. Štěpek and H. Daoust, "Lubricants and mold-release agents," in *Additives for Plastics*. New York, NY: Springer New York, 1983, pp. 34–49. DOI: [10.1007/978-1-4419-8481-4_3](https://doi.org/10.1007/978-1-4419-8481-4_3).
- [21] V. Karbhari, "Effect of internal mold release agent on the cure and property variation in resin transfer molding composites," *Journal of materials science letters*, vol. 17, no. 24, pp. 2061–2062, 1998.
- [22] R. Francis, "Ecoprofiles of recycled polymers at glance," in *Recycling of polymers: methods, characterization and applications*, 1st ed. Weinheim, Germany: Wiley-VCH, 2016, ch. 9, pp. 235–255.
- [23] R. Francis, "Methods of recycling," in *Recycling of polymers: methods, characterization and applications*, 1st ed. Weinheim, Germany: Wiley-VCH, 2016, ch. 3, pp. 55–114.
- [24] R. Francis, "Common additives used in recycling of polymers," in *Recycling of polymers: methods, characterization and applications*, 1st ed. Weinheim, Germany: Wiley-VCH, 2016, ch. 2, pp. 11–54.

- [25] A. Schulte, B. Kampmann, and C. Galafton, “Measuring the Circularity and Impact Reduction Potential of Post-Industrial and Post-Consumer Recycled Plastics,” *Sustainability*, vol. 15, no. 16, p. 12 242, Aug. 2023. DOI: 10.3390/su151612242.
- [26] S. Gohil, S. Suhail, J. Rose, T. Vella, and L. Nair, “Chapter 8 - polymers and composites for orthopedic applications,” in *Materials for Bone Disorders*, S. Bose and A. Bandyopadhyay, Eds., Academic Press, 2017, ch. 8, pp. 349–403. [Online]. Available: <https://www.sciencedirect.com/science/article/pii/B9780128027929000082> (visited on 02/12/2025).
- [27] *What is Plasma*, publisher: Plasmatrete. [Online]. Available: <https://www.plasmatrete.com/en/what-is-plasma> (visited on 01/22/2025).
- [28] *Plasmaplus®: Selective plasma coating in all different types of application*, publisher: Plasmatrete. [Online]. Available: <https://www.plasmatrete.com/en/technology/plasma-coating> (visited on 03/05/2025).
- [29] *Limning | RISE*, sv. [Online]. Available: <https://www.ri.se/sv/expertisomraden/expertis/limning> (visited on 01/27/2025).
- [30] N. Mostofi Sarkari, Ö. Doğan, E. Bat, M. Mohseni, and M. Ebrahimi, “Tethering vapor-phase deposited glymo coupling molecules to silane-crosslinked polyethylene surface via plasma grafting approaches,” *Applied Surface Science*, vol. 513, pp. 1–2, 2020. DOI: <https://doi.org/10.1016/j.apsusc.2020.145846>.
- [31] C. Deyá, “Silane as adhesion promoter in damaged areas,” *Progress in Organic Coatings*, vol. 90, p. 28, 2016. DOI: <https://doi.org/10.1016/j.porgcoat.2015.09.001>.
- [32] H. Szramowski and M. P. Krzemiński, “Comparative analysis of primers and alternative polypropylene pre-treatment techniques,” *The Journal of Adhesion*, vol. 100, no. 10, pp. 867–889, 2024. DOI: 10.1080/00218464.2023.2276110.
- [33] *SITA CleanoSpector - Inspecting parts cleanliness - SITA Messtechnik*, publisher: SITA. [Online]. Available: <https://www.sita-messtechnik.de/en/products/sita-cleanospector> (visited on 01/22/2025).
- [34] *SITA CleanoSpector Handheld Metal Cleanliness Test Instrument*, publisher: Dyne Testing. [Online]. Available: <https://dynetesting.com/product/sita-cleanospector-handheld-metal-cleanliness-test-instrument/> (visited on 01/22/2025).
- [35] E. S. Aydin, I. Korkut, and S. Ozbay, “Estimation of the Surface Free Energy Components for Solid Surfaces: A Machine Learning Approach,” en, *Arabian Journal for Science and Engineering*, vol. 49, no. 6, pp. 7863–7882, Jun. 2024. DOI: 10.1007/s13369-023-08502-4.
- [36] A. Rudawska and E. Jacniacka, “Analysis for determining surface free energy uncertainty by the owen–wendt method,” *International Journal of Adhesion and Adhesives*, vol. 29, no. 4, pp. 451–457, 2009. DOI: <https://doi.org/10.1016/j.ijadhadh.2008.09.008>.
- [37] B. Kronberg, K. Holmberg, and B. Lindman, *Surface chemistry of surfactants and polymers*. Chichester, West Sussex: Wiley, 2014, pp. 377–379.

- [38] D. Packham, "Surface energy, surface topography and adhesion," en, *International Journal of Adhesion and Adhesives*, vol. 23, no. 6, pp. 437–448, Jan. 2003. DOI: 10.1016/S0143-7496(03)00068-X.
- [39] N. Encinas, J. Abenojar, and M. Martínez, "Development of improved polypropylene adhesive bonding by abrasion and atmospheric plasma surface modifications," *International Journal of Adhesion and Adhesives*, vol. 33, pp. 1–6, Mar. 2012. DOI: 10.1016/j.ijadhadh.2011.10.002.
- [40] A. Jones, S. E. Davies, and K. Li, "Non-destructive surface roughness analysis for polymer-based products: Integrating laser speckle contrast and stylus profilometry," in *2024 IEEE International Conference on Manipulation, Manufacturing and Measurement on the Nanoscale (3M-NANO)*, Jul. 2024, pp. 344–349. DOI: 10.1109/3M-NANO61605.2024.10769643.
- [41] A. Rudawska, "Mechanical treatment," in *Surface Treatment in Bonding Technology*, A. Rudawska, Ed., Academic Press, 2019, pp. 87–128. DOI: <https://doi.org/10.1016/B978-0-12-817010-6.00005-9>.
- [42] F. Campbell, "Chapter 8 - adhesive bonding and integrally cocured structure: A way to reduce assembly costs through parts integration," in *Manufacturing Processes for Advanced Composites*, F. Campbell, Ed., Amsterdam: Elsevier Science, 2004, ch. 8, pp. 241–301. [Online]. Available: <https://www.sciencedirect.com/science/article/pii/B9781856174152500095> (visited on 01/30/2025).
- [43] S. Ebnesajjad, "Introduction and Adhesion Theories," in *Adhesives technology handbook*, 2nd ed, Norwich, NY: William Andrew Pub, 2008, ch. 1, pp. 1–19.
- [44] G. Malucelli, A. Priola, F. Ferrero, A. Quaglia, M. Frigione, and C. Carfagna, "Polyurethane resin-based adhesives: Curing reaction and properties of cured systems," *International Journal of Adhesion and Adhesives*, vol. 25, no. 1, pp. 87–91, 2005. DOI: <https://doi.org/10.1016/j.ijadhadh.2004.04.003>.
- [45] D. Segura, A. Nurse, A. McCourt, R. Phelps, and A. Segura, "Chapter 3 chemistry of polyurethane adhesives and sealants," in *Adhesives and Sealants*, ser. Handbook of Adhesives and Sealants, P. Cognard, Ed., vol. 1, Elsevier Science Ltd, 2005, pp. 101–162. DOI: [https://doi.org/10.1016/S1874-5695\(02\)80004-5](https://doi.org/10.1016/S1874-5695(02)80004-5).
- [46] *Polyuretan*, in Nationalencyklopedin AB. [Online]. Available: <https://www.ne.se/uppslagsverk/encyklopedi/l%C3%A5ng/polyuretan> (visited on 01/23/2025).
- [47] J. Aurrekoetxea, M. Sarrionandia, I. Urrutibeascoa, and M. L. Maspoch, "Effects of recycling on the microstructure and the mechanical properties of isotactic polypropylene," *Journal of materials science*, vol. 36, pp. 2607–2613, 2001. DOI: 10.1023/A:1017983907260.
- [48] K. Sanguanwong, M. Nikzad, I. Sbarski, and S. H. Masood, "Polymeric feedstock from post-consumer and post-industrial plastic wastes for automotive interior applications," *IOP Conference Series: Materials Science and Engineering*, vol. 455, p. 012048, Dec. 2018. DOI: 10.1088/1757-899X/455/1/012048.
- [49] B. A. Morris, "13 - effect of processing on quality," in *The Science and Technology of Flexible Packaging*, ser. Plastics Design Library, B. A. Morris, Ed., Oxford: William Andrew Publishing, 2017, pp. 465–513. DOI: <https://doi.org/10.1016/B978-0-323-24273-8.00013-7>.

A

Appendix 1



(a) PP Plasma Initial



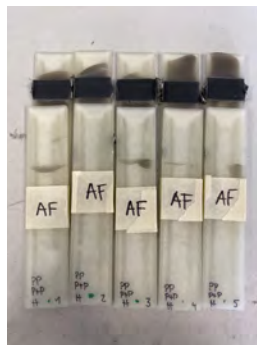
(b) PP Plasma Heat



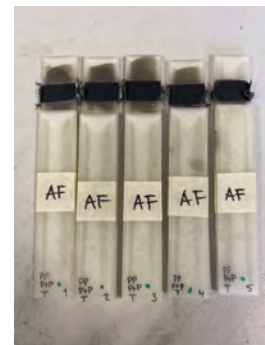
(c) PP Plasma Tropical



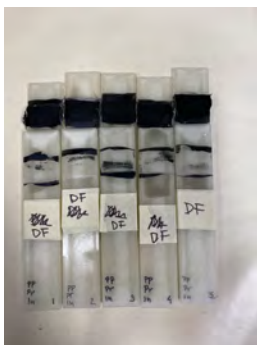
(d) PP Precursor Initial



(e) PP Precursor Heat



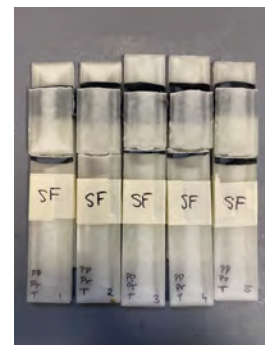
(f) PP Precursor Tropical



(g) PP Primer Initial



(h) PP Primer Heat

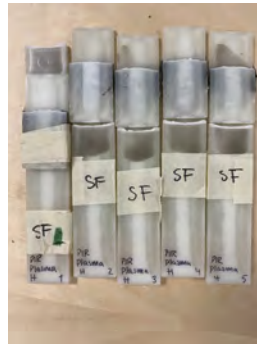


(i) PP Primer Tropical

Figure A.1: Pictures of the different failure modes from all the series of PP.



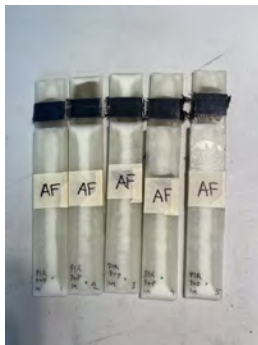
(a) PIR30 Plasma Initial



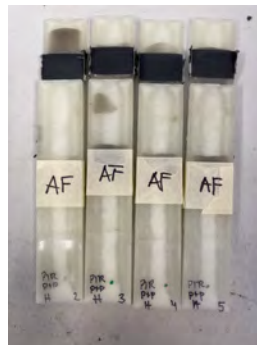
(b) PIR30 Plasma Heat



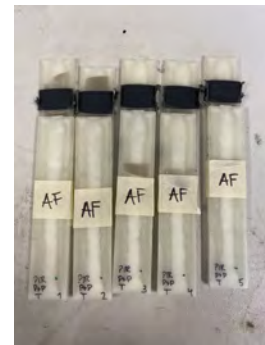
(c) PIR30 Plasma Tropical



(d) PIR30 Precursor Initial



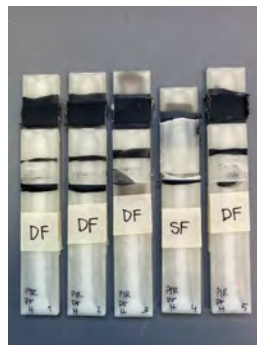
(e) PIR30 Precursor Heat



(f) PIR30 Precursor Tropical



(g) PIR30 Primer Initial



(h) PIR30 Primer Heat



(i) PIR30 Primer Tropical

Figure A.2: Pictures of the different failure modes from all the series of PIR30.



(a) PCR30 Plasma Initial



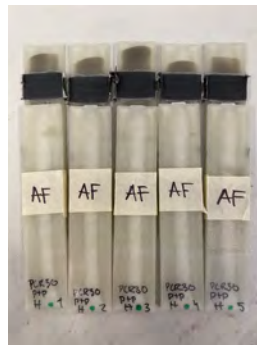
(b) PCR30 Plasma Heat



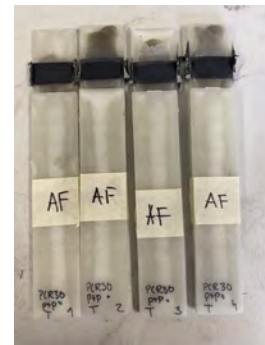
(c) PCR30 Plasma Tropical



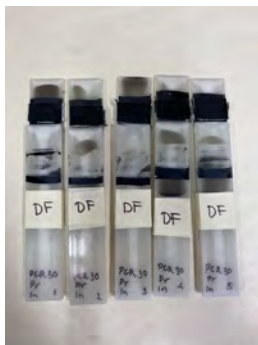
(d) PCR30 Precursor Initial



(e) PCR30 Precursor Heat



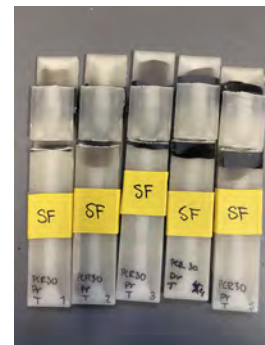
(f) PCR30 Precursor Tropical



(g) PCR30 Primer Initial



(h) PCR30 Primer Heat



(i) PCR30 Primer Tropical

Figure A.3: Pictures of the different failure modes from all the series of PCR30.



(a) PCR50 Plasma Initial



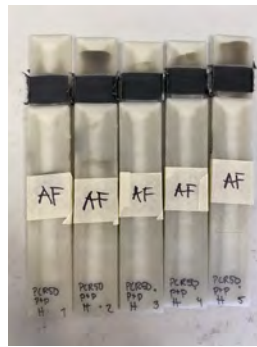
(b) PCR50 Plasma Heat



(c) PCR50 Plasma Tropical



(d) PCR50 Precursor Initial



(e) PCR50 Precursor Heat



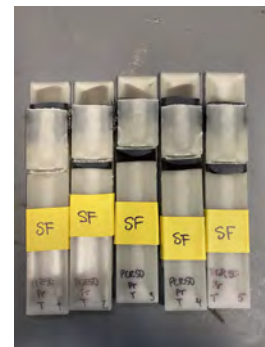
(f) PCR50 Precursor Tropical



(g) PCR50 Primer Initial



(h) PCR50 Primer Heat



(i) PCR50 Primer Tropical

Figure A.4: Pictures of the different failure modes from all the series of PCR50.

DEPARTMENT OF CHEMISTRY AND CHEMICAL ENGINEERING
CHALMERS UNIVERSITY OF TECHNOLOGY

Gothenburg, Sweden

www.chalmers.se



CHALMERS
UNIVERSITY OF TECHNOLOGY